December 2022

Generating Binder Inputs In Pavement ME For North Dakota's Conditions

Andebut Tilahun Yeneneh

GENERATING BINDER INPUTS IN PAVEMENT ME FOR NORTH DAKOTA'S CONDITIONS

by

Andebut Tilahun Yeneneh

Bachelor of Science in Civil Engineering, Addis Ababa University, 2016

A Thesis
Submitted to the Graduate Faculty

of the

UNIVERSITY OF NORTH DAKOTA

in partial fulfillment of the requirements

for the degree of

Master of Science
Civil Engineering
College of Engineering and Mines

Grand Forks, North Dakota

December

2022

Name: Andebut Yeneneh

Degree: Master of Science

This document, submitted in partial fulfillment of the requirements for the degree from the University of North Dakota, has been read by the Faculty Advisory Committee under whom the work has been done and is hereby approved.

DocuSigned by:
Daba Gedafa
F92218D8FFDA4FC...
Daba Gedafa

DocuSigned by:
Nabil Suleiman
6437D86DC3B542E...
Nabil Suleiman

DocuSigned by:
Bruce Dockter
FE2911F7AA5C4CF...
Bruce Dockter

This document is being submitted by the appointed advisory committee as having met all the requirements of the School of Graduate Studies at the University of North Dakota and is hereby approved.

DocuSigned by:
Chris Nelson
2E0AF088C733403...
Chris Nelson
Dean of the School of Graduate Studies

12/7/2022
Date

PERMISSION

Title**:** Generating Binder Inputs in Pavement ME for North Dakota's Conditions

Department Civil Engineering

Degree Master of Science (MSc.)

In presenting this thesis in partial fulfillment of the requirements for a graduate degree from the University of North Dakota, I agree that the Library of this University shall make it freely available for inspection. I further agree that permission for extensive copying for scholarly purposes may be granted by the professor who supervised my thesis work or, in his absence, by the Chairperson of the department or the dean of the School of Graduate Studies. It is understood that any copying or publication or other use of this thesis or part thereof for financial gain shall not be allowed without my written permission. It is also understood that due recognition shall be given to me and to the University of North Dakota in any scholarly use which may be made of any material in my thesis.

Andebut Yeneneh

12/07/22

TABLE OF CONTENTS

LIST OF FIGURES

LIST OF TABLES

ACKNOWLEDGEMENTS

First of all, I would like to thank God Almighty for giving me the opportunity and guidance to achieving my goal and to be successful in this journey. My most profound appreciation goes to Daba Gedafa, Ph.D., P.E., ENV SP, F. ASCE, my advisor, for his guidance, support, and understanding in helping me succeed in my studies as well as for giving me the opportunity to work on North Dakota Department of Transportation (NDDOT) funded project. In addition, I'd like to thank my academic committee members, Dr. Nabil Suleiman, and Mr. Bruce Dockter, for academic guidance and technical assistance throughout my research. I am highly indebted to UND and UND Civil Engineering Faculty for providing all the necessary materials and information necessary for the completion of this thesis.

DEDICATION

I dedicate this to my loving and caring family and beloved friends for all the support they provided me.

ABSTRACT

There is a broad consensus that the current mechanistic-empirical pavement design guideline (MEPDG) is an improvement from the earlier empirical-based design approaches. The lack of comprehensive material input databases for bound and unbound layers remains challenging. This study developed a database for binders used in typical hot mix asphalt (HMA) mixes in North Dakota by measuring their complex shear modulus (|G*|) and associated phase angle (δ) at unaged, short-term aged, and long-term aged conditions. Binder viscosity was also measured in these three aged states. Additionally, this study used existing models to predict (|G*|) and δ and compared them to measured values. Results illustrated that the aging effect increased binder viscosity; however, the values remained within the viscoelastic range. The |G*| and δ values for the unaged and short-term aged binders revealed that all the binders performed satisfactorily at high temperatures according to their performance grades. For unaged binders, the PG58H-34 for Highway (HWY) 83 and HWY 32 displayed different |G*| and δ values indicating the importance of undertaking local binder characterization. For short-term aged binders, PG 58H-34-HWY 83 showed high stiffness and high elasticity at high temperatures indicating that it is suited for pavements carrying heavy traffic. |G*| values increased significantly with long-term aging, with HWY 32 PG 58S-28 displaying the highest stiffness indicating a higher susceptibility to fatigue cracking in the future. Comparing the predicted and measured short-term aged |G*| and δ for the eight binders revealed mixed results. R^2 values above 0.9 for predicted and measured |G*| for all the binders were observed, while for six binders, the R^2 values were above 0.8 for predicted and measured δ, and for two binders, the R^2 values were below 0.5. Using measured A and VTS values instead of default values is recommended as a remedy for poor phase angle predictions. Using the |G*|/sinδ parameter showed that PG 58H-34-HWY 94 had the highest rutting resistance, while the Multiple Stress Creep Recovery (MSCR) test showed that PG 58S-34-HWY 1was the most rut-

resistant binder. |G*|. sin(δ) parameter indicated that PG58H-34-HWY 52 had the highest fatigue resistance, while the Linear Amplitude Sweep (LAS) test indicated that PG 58H-34-HWY 94 had the highest fatigue resistance. The binder ranking results did not match, meaning that further testing is required with the inclusion of independent tests to verify the rankings.

KEYWORDS: binder characterization, complex shear modulus, phase angle, viscosity, prediction, Pavement ME.

CHAPTER I

INTRODUCTION

1.1 General

At 93 percent, asphalt pavements are the most common type of pavement in the United States (Hossain et al., 2013). Asphalt pavements are layered structures, with the top - most layer made of asphalt binder, an end product of petroleum crude oil and unbound materials from natural deposits of sand or gravel from quarries. Asphalt pavements are considered economical to construct since mostly cheap and locally available materials are used. This layer is subjected to direct traffic and environmental loads; therefore, asphalt binder quality dictates the ultimate performance of the flexible pavement structure.

Asphalt binder is a viscoelastic material whose behavior is dictated by temperature (T) and loading rate (f). Due to its complex nature, selecting an appropriate asphalt binder is a significant step in asphalt pavement construction. Physical and rheological properties are commonly used criteria for selecting and grading asphalt binders. Several asphalt grading systems exist, the most common being penetration grading, viscosity grading, and Superpave performance grading (PG) (Ghuzlan & Al-Khateeb, 2013). The Superpave PG testing designed by the Strategic Highway Research Program (SHRP) specifies the binders' properties according to applied temperature and loading conditions. The Superpave PG system is the most recent, and 49 states in the US have implemented its use in the selection of asphalt binders in their road projects (Hossain et al., 2013).

The selection of PG asphalt binders is expected to satisfy binder aging and environmental conditions reliably; consequently, the PG system employs a conventional testing regimen that measures the binder's physical characteristics that can be directly linked to performance in the

field. PG system grading ensures that the selected binder meets all required criteria by Pavement ME methods for flexible pavement design.

Researchers have established that the 1993 American Association of State Highway and Transportation Officials (AASHTO) Guide is inadequate in estimating the complicated failure mechanisms of asphalt pavements (Zhang et al., 2000). Empirical equations from the American Association of State Highway Officials (AASHO) Road Test form the basis of this guide, meaning that it is most effective in situations matching the test conditions (Li et al., 2011). Currently, performance methods that can measure pavement distress directly from the pavement surface are gaining acceptance. The MEPDG was developed to integrate mechanistic methods, local materials, local climate, and traffic conditions to improve pavement design (ARA, 2004).

Several states have developed such material input databases in preparation for Pavement ME implementation (Birgisson et al., 2004; Gedafa et al., 2010; Mohammad et al., 2014). The Pavement ME requires a comprehensive material input database for successful implementation; therefore, local material characterization is necessary. Determining asphalt properties is essential for achieving strong and durable flexible pavements. The measurement of these binder properties was the subject of this research.

1.2 Problem Statement

The AASHO conducted road tests in Ottawa, Illinois, at the end of the 1950s to establish a tax mechanism for various vehicle classes based on gas usage. The AASHTO used the test section's data and performance history to develop the 1972 AASHO design guide. The organization then updated its guides to the 1986 and 1993 AASHTO guides for the design of pavement structures. The calculation models adopted in the 1993 design guide were based on the initial AASHO road test conditions. The experimental nature of these equations is a significant limitation since

fundamental material properties are not considered. Additionally, the AASHO road tests were conducted under single climatic conditions and subgrade types of Ottawa City, with materials specifications, mixture designs, and traffic inputs bound to Illinois and 1950s engineering practice. The National Cooperative Highway Research Program (NCHRP) project 1-37A addressed these limitations by developing a novel pavement design methodology. This guide defined the use of ME methods that consider local conditions and material properties used in construction. The ME approach employs engineering mechanics to calculate pavement responses, such as stresses, strains, and deflections, and the empirical models for predicting pavement performance.

Although there is a broad consensus that the ME approach to designing pavement structures is an improvement from the earlier empirical-based design approaches, critical implementation challenges remain. One is the lack of comprehensive material input databases for bound and unbound layers. Consequently, to implement the ME design approach, State Highway Agencies (SHAs) must undertake extensive laboratory tests that are costly and time-consuming. Developing a database for typical binders for North Dakota is a step forward in overcoming this challenge and enhancing the application of the ME design approach in the state.

This study aimed to develop Level 1 libraries of inputs for typical binders in North Dakota. There are three levels of input in pavement ME. Level 1, the most accurate, involves determining asphalt binder properties and mixes in the laboratory. A combination of laboratory-determined and predicted mix and binder properties are used at Level 2. Predicted and default values were used at Level 3, which is the least accurate. Prediction models that provide estimated properties comparable to laboratory binder and mix test results were recommended for future use to reduce the number of laboratory tests.

1.3 Objectives

The main objectives of this study were to:

- Measure viscosity, complex shear modulus, and phase angle of binders used in typical North Dakota HMA mixtures.
- Predict the complex shear modulus and phase angle of the binders used in typical HMA mixes in North Dakota and compare them to laboratory test results.
- Evaluate the effectiveness of Linear Amplitude Sweep (LAS) and Multiple Sweep Creep Recovery (MSCR) tests in measuring fatigue cracking and rutting resistance, respectively.

1.4 Methodology

This research contains two parts; the first focuses on extensive laboratory tests to characterize the properties of binders used in typical HMA mixes in North Dakota. Binders were collected from eight different project sites around North Dakota. The rheological properties of the eight binders were determined by measuring the complex shear modulus, phase angle, and viscosity at different aging stages. The second part deals with predicting these rheological properties using established models to provide an effective tool that can substitute the costly and time-consuming laboratory experiments. Detailed experimental plans and predictions are further discussed in the methodology section. The test results and prediction results are analyzed and discussed after that.

1.5 Organization of Thesis

Chapter I provides a background on binder properties and the primary goal of the research. Chapter II describes the rheological properties of binders and discusses the prediction of viscosity, complex shear modulus, and phase angle. Chapter III covers the experimental plan for original, short-term aging, and long-term aging. This chapter covers the two major rheological binder properties,

complex shear modulus and phase angle measuring methodology, in detail. Binder viscosity, a parameter that indicates the behavior of the asphalt concrete during production and construction, is also discussed. Binder ranking according to rutting and fatigue cracking susceptibility using MSCR and LAS tests will be covered. Chapter IV presents a discussion of the analysis and results of the experimental and prediction results. Finally, the conclusions, recommendations, limitations, and future work are incorporated in Chapter V.

CHAPTER II

LITERATURE REVIEW

2.1 General

Asphalt pavements in cold regions such as North Dakota experience extreme environmental conditions that result in various pavement distresses and ultimately reduce their service life. Asphalt binder imparts most of its properties to the asphalt mixture, meaning that understanding binder properties is integral in estimating long-term pavement performance. This chapter presents literature on important binder properties and testing methods that will be applied to this study.

2.2 Binder Properties

Asphalt binder's properties mainly govern the mechanical performance of asphalt concrete, making its characterization an essential step in the ME design approach (Yu & Shen, 2013). Asphalt binder is a thermoplastic material that displays linear viscoelastic (LVE) behavior under in-service pavement operating conditions (Dondi et al., 2014). The LVE properties of asphalt binders are represented as the complex modulus |G*| and the phase angle (δ), which are measurements of the relationship between stress and strain of the binder under varying temperatures and loading time (Dondi et al., 2014). These two parameters are indicators of the binder's elasticity and viscosity under these varying conditions.

Viscosity is another essential property of the asphalt binder that gives indications of its pumpability, workability, and mixability, all of which are integral in producing acceptable asphalt concrete. These three properties of the asphalt binder are discussed further in the following section.

2.2.1 Complex Modulus |G*| and Phase Angle (δ)

|G*| is an indicator of the resistance to deformation of an asphalt binder and is defined by Equation 2-1:

$$|G^*| = \frac{\tau_{Max}}{\gamma_{Max}} \quad (2\text{-}1)$$

where τ_{Max} is the absolute value of the peak-to-peak shear stress and γ_{Max} is the absolute value of the peak-to-peak shear strain (Dondi et al., 2014). The phase angle, on the other hand, is the time lag (Δt) between the applied shear stress and the resulting shear strain converted into degrees, as shown in Equation 2-2.

$$\delta = \frac{\Delta t}{t} .360 \quad (2\text{-}2)$$

where t is the loading time.

Several reports have emphasized the importance of the |G*| and δ values in providing early indications of the performance of the asphalt mix to be produced (Dondi et al., 2014; Yusoff et al., 2011; Li et al., 2019), and others. The general agreement is that these two parameters are key inputs in the application of the ME pavement design approach and therefore need to be determined during the earlier stages of the design.

The |G*| and δ values can be determined experimentally, empirically, or through numerical modelling (Yu & Shen, 2013). Since this project aims to prepare level 1 library inputs, laboratory experiments were carried out to measure the |G*| and δ values of the sample asphalt binders provided by the NDDOT.

The dynamic shear rheometer (DSR) is the recommended equipment for determining the viscoelastic properties of an asphalt binder because of its ability to measure |G*| and δ values under varying temperatures and frequencies (Yusoff et al., 2011). The DSR was used to determine the |G*| and δ values in accordance with AASHTO T315 for level 1 and 2 inputs (Li et al., 2019).

For level 3 inputs, the A-VTS viscosity-temperature susceptibility parameters based on the Superpave PG system were employed.

2.2.2 Viscosity (η)

An asphalt binder's viscosity indicates the asphalt mix's behavior during production and construction. Specifically, an asphalt mix's pumpability, mixability, and workability are properties governed by the asphalt binder's viscosity used in the mix preparation (Colbert & You, 2012).

An asphalt binder's viscosity can be measured in the laboratory through various methods; however, the Brookfield rotational viscometer apparatus is the preferred choice for this project due to its advantages in measuring the viscosity of materials display viscoelastic properties such as asphalt binders (Colbert & You, 2012). This project utilized this method to determine the viscosity of original, short-term aged, and long-term aged binders following AASHTO R 28(AASHTO, 2021).

2.2.3 Binder Characterization for Pavement ME

Several states have measured |G*|, δ, and η to develop binder inputs to support their pavement ME implementation. Ape Agyei & Diefenderfer (2011) measured the |G*| and δ for 18 Virginia asphalt concrete mixtures to evaluate and present the binder properties in a format that could be assimilated into their pavement ME. The asphalt binders were recovered from plant mixes, and DSR was used to determine the rheological properties of the recovered binders at multiple temperatures and a frequency of 10 rad/sec. These tests enabled the determination of actual binder PG grades and stiffness.

Awed et al. (2011) evaluated the effect of viscosity-based and G*- based models to predict Dynamic modulus (E*) for levels 2 and 3 of the pavement ME. The study measured 22 HMA mixtures typically used in Idaho with six binder grades. Viscosity data were obtained using the

Brookfield viscometer, while |G*| and δ data were obtained using the DSR. Their results revealed that both E* models produced acceptable E* predictions. The authors recommended the need for conducting localized binder characterization as a means of evaluating E* prediction for MEPDG implementation.

Birgisson et al. (2004) conducted the E* testing of 28 HMA mixtures typically used in Florida. They developed predictive models to compare with their measured data. Their results showed that predictive models that used input viscosities from the DSR underestimated E* values as compared to laboratory values. Their results demonstrated that binder inputs had an effect on viscosity-based and G*-based E* predictions, and emphasis was given to local binder characterization as a means of achieving accurate results.

The literature review demonstrates that binder properties are critical in determining the E* of HMA mixes. The type of binder property is an essential characteristic in determining the outcome of the predictive models. Each state should conduct its own binder characterization to enable the accurate prediction of E* in support of the Pavement ME implementation.

2.3 Prediction of Viscosity, Complex Shear Modulus, and Phase Angle

The MEPDG uses asphalt binder viscosity as a primary input parameter in all three hierarchical levels (Bari & Witczak, 2007). The ASTM A_i-VTS_i viscosity model Equation 2-3 is used to obtain the design viscosity when applying the MEPDG. The model compares binder viscosity to temperature in the Rankine scale as shown in Equation 2-3:

$$loglog(\eta) = A + VTS.\log(T_R) \tag{2-3}$$

where

η = viscosity (cP),

T_R= temperature (degree Rankine),

A = regression intercept, and

VTS = regression slope (viscosity-temperature susceptibility parameter).

Table 2.1 Default Values of A and VTS Based on Asphalt PG (ARA, 2004).

PG	A	VTS
52-28	11.84	-4.012
58-28	11.01	-3.701
52-34	10.707	-3.602
52-40	9.496	-3.164
64-34	9.461	-3.134

Pavement ME's levels 1 and 2 require laboratory measurement as inputs, which are converted to viscosity and fitted into the model by use of statistical regression methods (Bari & Witczak, 2007); however, for level 3, the MEPDG default A and VTS values listed in Table 2.1 used to estimate binder viscosity. The binder viscosity calculated at all three levels ignores the loading rate. A fixed binder viscosity is assumed at changing loading rates, which is inaccurate, especially at low to medium temperature ranges (Bari & Witczak, 2007).

Bari & Witczak (2007) developed a modified version of the ASTM A_i-VTS_i model by considering the loading rate effect on viscosity. Using two frequency adjustment factors the regression intercept A and the slope VTS were modified for loading frequency and introduced into Equation 2-3. The modified ASTM A_i-VTS_i equation (Equation 2-4) was thus presented in its final form:

$$loglog\ \eta_{f_s,T} = c_0 f_s^{c_1} xA + d_0 f_s^{d_1} xVTS.\log(T_R) \quad (2\text{-}4)$$

where

$\eta_{f_s,T}$= viscosity of asphalt binder as a function of both loading frequency (f_s) and temperature (T), (cP),

f_s =loading frequency in dynamic shear modulus as used in the G_b^* testing (*Hz*),

A= regression intercept from the conventional ASTM A_i -VTS_i equation (Equation 2-3),

VTS= regression slope (viscosity-temperature susceptibility parameter) (Equation 2-3),

c_0 and c_1 = frequency adjustment factor for A, functions of f_s and T,

d_0 and d_1 = frequency adjustment factor for VTS, functions of f_s and T, and

T_R= temperature (degree Rankine)

Apart from the modified ASTM A_i -VTS_i model, Bari & Witczak (2007) developed two other models: one for estimating the binder's shear complex modulus ($|G_b^*|$), and the other for estimating the phase angle (δ_b) associated with G_b^*. The models' final forms are presented as Equations 2-5 and 2-6, respectively:

$$|G_b^*| = 0.0051 f_s \eta_{f_s,T} (sin\delta)^{7.1542 - 0.4929 f_s + 0.0211 f_s^2} \quad (2\text{-}5)$$

where,

$|G_b^*|$= dynamic shear modulus (*Pa*),

f_s= dynamic shear loading frequency to be used with $|G_b^*|$ and δ_b (*Hz*),

$\eta_{f_s,T}$= viscosity of asphalt binder as a function of both loading frequency (f_s) and temperature (T), (*cP*),

δ_b= phase angle (deg).

$$\delta_b = 90 + (b_1 + b_2 VTS')x log\left(f_s x \eta_{f_s,T}\right) + (b_3 + b_4 VTS')x\{\log (f_s x \eta_{f_s T})\}^2 \quad (2\text{-}6)$$

where,

δ_b= phase angle (deg),

f_s = dynamic shear loading frequency to be used with $|G_b^*|$ and δb (*Hz*),

VTS'= adjusted VTS,

$\eta_{f_s,T}$= viscosity of asphalt binder as a function of both loading frequency (f_s) and

temperature (T), (cP),

b_1, b_2, b_3, and b_4 = fitting parameters = -7.3146, -2.6162, 0.1124, and 0.2029.

Equations 2-4, 2-5, and 2-6 showed the capability to accurately predict the stiffness characteristics of most binders and HMA mixtures. The revised ASTM A_i –VTS_i viscosity model to was used to predict binder viscosity. The binder's dynamic shear modulus, associated phase angle at a specific temperature, and loading frequency from the A_i and VTS_i values were predicted.

2.4 Rutting

Rutting is a type of pavement distress that manifests as a depression along the wheelpath of an asphalt pavement and is likely to occur under repeated heavy traffic loading coupled with high temperatures (Figure 2.1). Binder stiffness plays a significant role in rutting resistance, and its characterization helps in selecting the suitable binder that corresponds to a region's traffic and environmental loading (Wang et al., 2021).

Figure 2.1 Rutting Distress in Asphalt Pavements (Wang et al., 2021).

2.4.1 Binder Grading for Rutting Resistance

A rutting-resistant asphalt binder is characterized by a combination of stiffness and elasticity, which enables it to resist deformation while being able to rebound to its original shape. |G*|/sinδ is a parameter obtained from binder grading that indicates the stiffness and elastic components of the asphalt binder. Equation 2-7 depicts an interpretation of the |G*|/sinδ parameter where rutting is viewed as a resultant of cyclic loading. The work done to deform the asphalt pavement is partly regained by the elastic rebound of the pavement and partly dissipated by rutting. The |G*|/sinδ parameter should be maximized to minimalize rutting. The work dissipated per loading cycle at a constant stress can be expressed as Equation 2-7 (Yao et al., 2012).

$$W_c = \pi\sigma_0^2 \left[1/(\frac{G^*}{\sin\delta})\right] \quad (2\text{-}7)$$

where,

W_c = work dissipated per load cycle,

σ = stress applied during load cycle,

G^* = complex modulus,

δ = phase angle.

Superpave PG system specifies a minimum threshold value for |G*|/sinδ at 1.0 kPa and 2.2 kPa for unaged and RTFO-aged asphalt binders, respectively (AASHTO, 2020).

2.4.2 Multiple Stress Creep Recovery (MSCR) Test

Research has revealed that the |G*|/sinδ parameter is inaccurate in grading the high-temperature performance of modified asphalt binders (Zeiada et al., 2022; D'Angelo et al., 2007) developed the MSCR test, which employs the creep and recovery model to examine the binder's ability to resist permanent deformation. The DSR is used to apply a 1s creep load to the binder specimen,

followed by a 9s recovery period. Figure 2.2 illustrates the typical behavior during the MSCR testing cycle. Testing commences by applying a low stress 0.1 kPa for 10 creep/recovery cycles, which is later raised to 3.2 kPa and repeated for an additional 10 cycles.

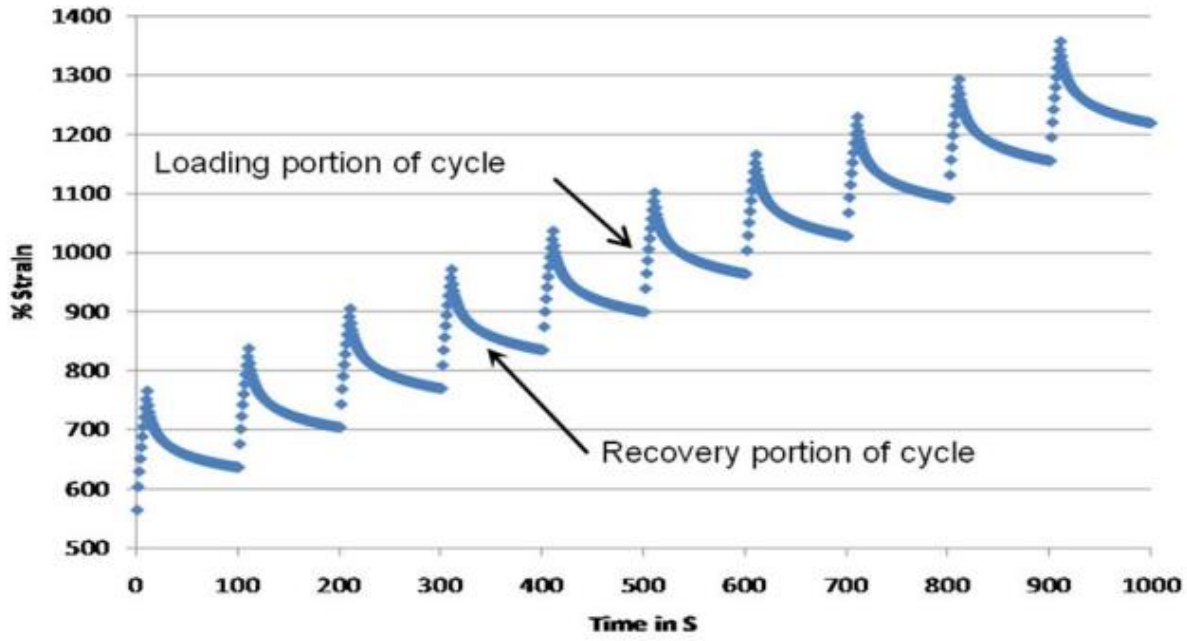

Figure 2.2 Evolution of Shear Strain with Time in the MSCR Test (FHWA, 2011).

The primary benefit of the MCSR test is to subject the asphalt binder to higher stress and strain levels as compared to the PG test parameter |G*|/sinδ; thereby capturing the stiffening behavior of the binder and delayed elastic effects (Zeiada et al., 2022). The MSCR test parameter "J_{nr}" is termed the non-recoverable creep compliance and is obtained by dividing the residual shear strain at the end of the recovery portion by the applied stress during the creep portion, as shown in Equation 2-8.

$$J_{nr}(\tau, N) = \frac{\Delta\gamma}{\tau} \quad (2\text{-}8)$$

where,

J_{nr} = non-recovered creep compliance

τ = creep stress

$\Delta\gamma$ = residual shear strain

The MSCR parameter J_{nr} has been shown to be an improved indicator of the rutting response of most binders as compared to |G*|/sinδ. This study evaluated the output of these two rutting indicators and ranked North Dakota's binders accordingly.

2.5 Fatigue Cracking

Fatigue cracking, commonly referred to as alligator cracking, is a type of pavement distress that occurs due to repeated traffic loading. Fatigue cracking is a common phenomenon in thin pavements, where cracking starts at the bottom of the asphalt layer due to higher tensile stresses, which gradually propagate to the top, forming one or multiple longitudinal cracks (Zeiada et al., 2022). This phenomenon is termed "bottom-up" cracking. This continuously repeated loading results in the interconnection of the cracks, as observed in Figure 2.3.

Figure 2.3 Fatigue Cracking (Alligator Cracking) in Asphalt Pavements (Wang et al., 2021).

2.5.1 Binder Grading for Fatigue Cracking Resistance

An asphalt binder needs to be elastic and moderately stiff to prevent cracking under repeated loading. The Superpave PG viscous parameter |G*|. sinδ needs to be minimized to prevent fatigue cracking. Equation 2-9 shows that the relationship between the work dissipated for every cycle is directly proportional to the |G*|.sinδ parameter. Therefore, to prevent cracking, the |G*|.sinδ parameter needs to be minimized, which will correspondingly reduce the energy dissipated (Hintz & Bahia, 2013).

$$W_c = \pi \varepsilon_0^2 [(G^*)(sin\delta)] \quad (2\text{-}9)$$

The Superpave PG specifies a maximum value of 5000 kPa for G*.sinδ values measured from DSR tests conducted on long-term aged asphalt binders.

2.5.2 Linear Amplitude Sweep (LAS) Test

The Superpave G*.sinδ parameter has a disadvantage since it can only evaluate the asphalt binder's fatigue resistance within the viscoelastic range. Therefore, the accurate evaluation of binders that display nonlinearity, especially modified binders, cannot be evaluated using the G*.sinδ parameter. Johnson & Bahia (2010) developed the LAS test, which incorporates the concept of damage accumulation as a means of measuring fatigue resistance. The LAS test is performed by applying oscillating shear loads, increasing the strain amplitude, and controlling the strain. The viscoelastic continuum damage (VECD) analyses the results. The analysis is carried out based on fatigue law parameters A and B. These two parameters are model coefficients that depend on asphalt binder properties. Generally, binders with high fatigue resistance display higher A and lower B values. The repetition of cycles to failure is determined using Equation 2-10, which calculates the fatigue failure of the asphalt binder (Hintz & Bahia, 2013).

$$Nf = A(\gamma max)\, B \quad (2\text{-}10)$$

Where,

Nf measures variation in pavement structure with changing maximum strain γmax. The strain level corresponds to traffic loading. Reports show that the binders' predicted fatigue resistance correlates well with fatigue cracking field measurements. The LAS test laid out in AASHTO TP 101 (AASHTO, 2014b) was used in this research to evaluate the fatigue resistance of long-term aged binders and compare the outcome with those from the G*.sinδ parameter.

CHAPTER III

METHODOLOGY

3.1 Experimental plan

The properties of binders used in typical mix in North Dakota HMA mixes were characterized by measuring their complex shear modulus, Phase angle, and viscosity for binders. The complex shear modulus (G*) and phase angle (δ) of the original, Rolling Thin Film Oven (RTFO) aged, and Pressure Aging Vessel (PAV) aged binders were determined by using DSR at a frequency of 10 rad/sec per AASHTO T315 specification. A Brookfield rotational viscometer was used to determine the viscosity of original, RTFO-aged, and PAV-aged binders according to AASHTO R 28 test protocol(AASHTO, 2021a).

For the original binder, the viscosity was measured using a viscometer and complex shear modulus and phase angle using DSR. For short term aged binder, original binder was put in RTFO to get short-term aged binder then measured complex shear modulus and phase angle. To get a long-term aged binder, the residue of the short-term aged binder was conditioned using PAV. Then complex shear modulus and phase angle were measured. The parameters used to characterize fatigue and rutting resistance of asphalt binder were also measured using the DSR. Figure 3.1 shows the overall experimental plan.

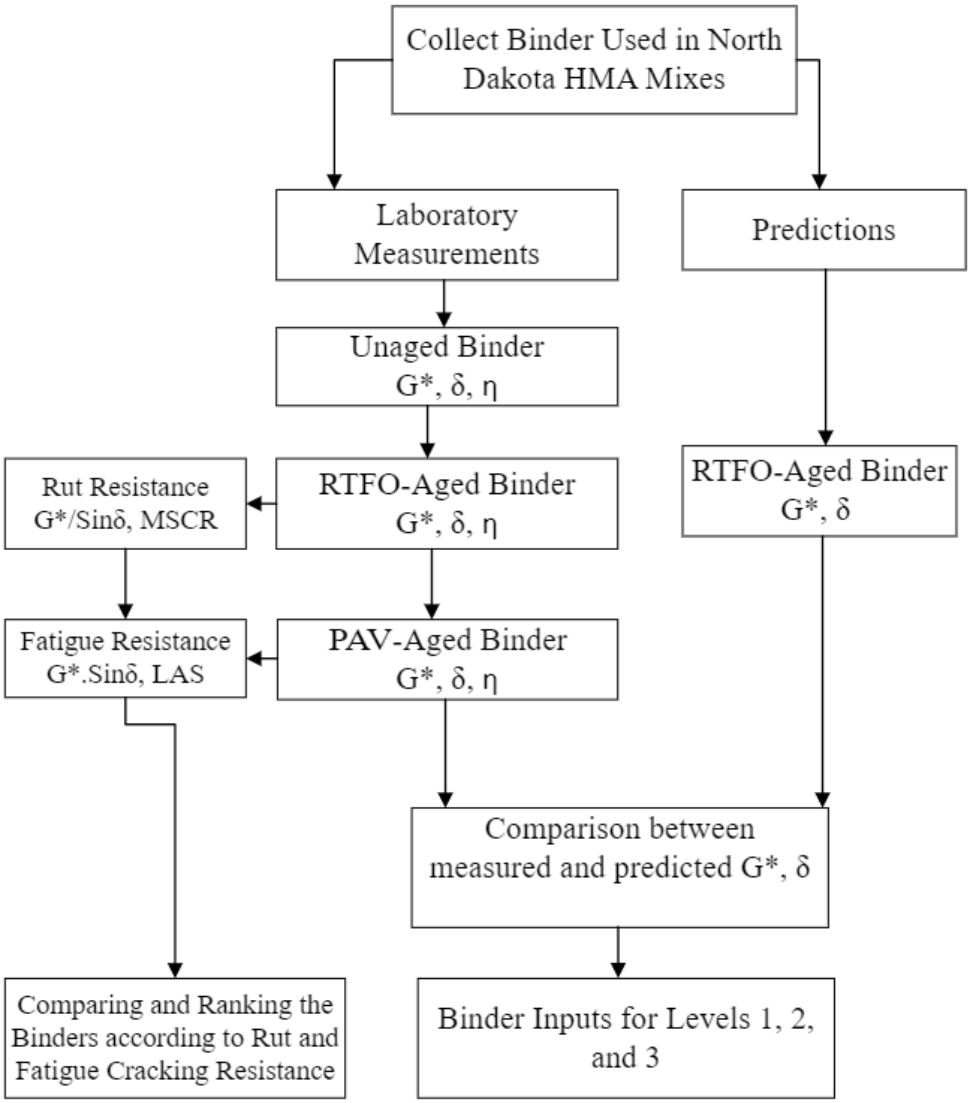

Figure 3.1 Experimental Plan.

3.2 Material Selection

Binder grades (PG 58S-28, 58H-28, 58S-34, and 58H-34) were collected from eight project sites in North Dakota. For each binder the viscosity, complex shear modulus, and phase angle were measured. For each test, 128 specimens were used.

3.3 Binder Preparation

This study investigated binder properties in unaged, short-term aged, and long-term aged conditions. Steric hardening occurs in asphalt when stored at room temperature over time;

therefore, the binders were heated at 145 ºC (290 ºF) for 4 hours before testing the binder for unaged conditions.

Short-term aging was achieved by using the RTFO whereby 35±0.5 g of the binder was placed in the oven for 85 minutes at 163 ºC (325ºF) following AASHTO T240-21 (AASHTO, 2021b).

Long-term aging is simulated in the laboratory by further aging of the short-term aged binder. A specimen weighing 50±0.5g was placed in the PAV for 20h ± 10 minutes and subjected to a temperature of 100 ºC (212ºF) at an air pressure of 2.1 ± 0.1 mPa according to AASHTO R 28-21- (AASHTO, 2021). Table 3.1 summarizes the tests conducted on the binders.

Table 3.1 Tests on Binders

No.	Binder Test	Binder type and Tests	Sample preparation	Number of specimens	Test Standard **(AASHTO)**
1.	DSR	Original	-	16	T315
		Short-term	RTFO	16	T315, R28
		Long-term	PAV	16	T315, T240
		MSCR	RTFO	16	TP70
		LAS	PAV	16	TP101
2.	Brookfield	Original	-	16	T324, D77241
		Short-term	RTFO	16	
		Long-term	PAV	16	

3.4 Binder Viscosity Test

Binder viscosity is an essential input in all three hierarchical levels of the MEPDG. In this research, a rotational viscometer was used to measure the viscosity of each binder at 135ºC according to AASHTO T316. To measure the relative resistance to rotation, torque is needed to keep up a

cylindrical spindle's constant rotation speed while immersed in a binder specimen at a constant temperature. The torque and rotation speed of cylindrical was used to obtain the viscosity in Pascal-seconds (Pa. s). The binders' viscosity should be below 3 Pa.s (ASTM, 2015). Figure 3.2 shows the viscometer used in this study.

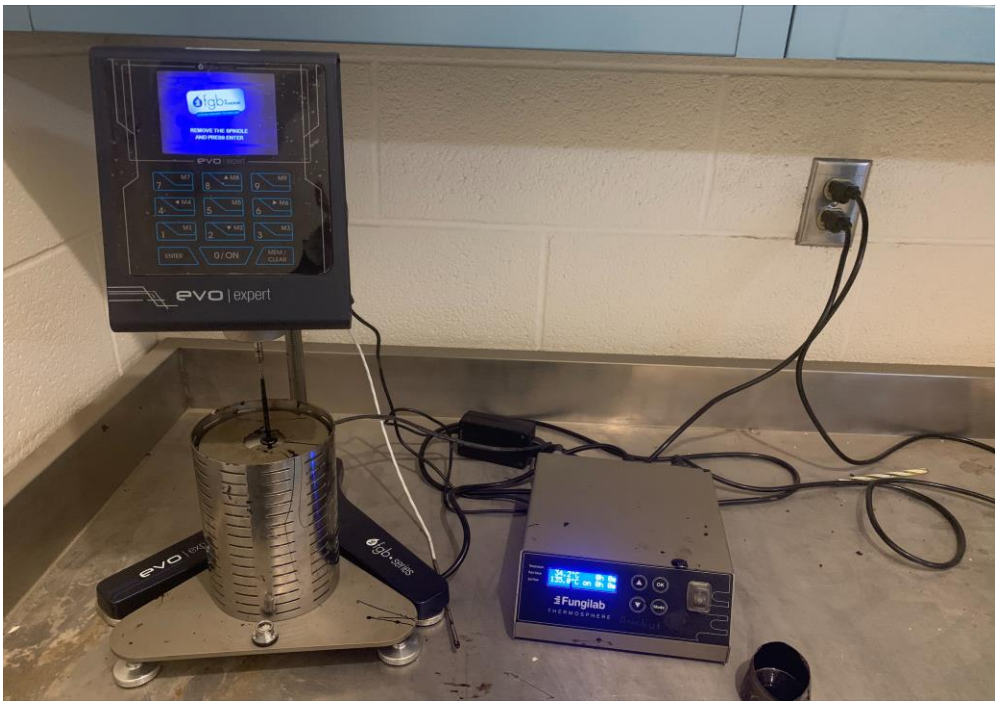

Figure 3.2 Viscometer

3.5 Rolling Thin Film Oven (RTFO)

Short-term aging was simulated using the RTFO according to AASHTO T240 (AASHTO, 2021b). The RTFO is an oven specially designed to heat and circulate air to speed up the short-term aging process of the asphalt binder (Figure 3.3). The RTFO simulates the condition of the asphalt binder properties change during the batch plant, drum mix plant, transportation of mix, and immediately after the flexible pavement is constructed (AASHTO, 2021b).

Figure 3.3 Rolling Thin-Film Oven (RTFO)

Asphalt binder measuring 35 ± 0.5 g was placed into a modified glass bottle after pouring, the bottle was cooled for 60 minutes on a cooling rack, as illustrated in Figure 3.4.

Figure 3.4 Pouring 35 ± 0.5g of Binder into each Container and Container Cooling on Sample Rack

After the specimens cooled down, the samples were placed in the RTFO for 85 minutes at 163oc(325oF). The residue from this test was tested according to AASHTO T 315 and conditioned in PAV for long-term aging simulation.

3.6 Pressurized Aging Vessel (PAV)

The PAV simulated the asphalt binders' long-term aging by exposing them to elevated temperature and pressure. An RTFO-aged binder residue of 50 ± 0.5 g was transferred to a PAV pan and put

into the preheated PAV. The elevated temperature was maintained at 100°C at a pressure of 2.1 ± 0.1 MPa for 20 h ± 10 minutes. After completion of the PAV aging, the PAV residue was heated at 163˚C to facilitate pouring. After the PAV conditioning process was completed, the samples were transferred to the DSR and viscometer for testing. Figure 3.5 shows the PAV vessel used for long-term aging.

Figure 3.5 Pressurized Aging Vessel (PAV)

3.7 Dynamic Shear Rheometer (DSR) Test

The DSR was used to characterize the viscous and elastic behavior of binders at varying temperatures and loading rates. The DSR used in this research is automated and uses proprietary software for running the test. Temperatures experienced in North Dakota were used as a guideline for selecting the asphalt binder testing temperatures. For North Dakota, intermediate temperature rheology was tested following AASTHO 315. The DSR was used to evaluate the rutting and fatigue resistance of the binders at the three aging conditions.

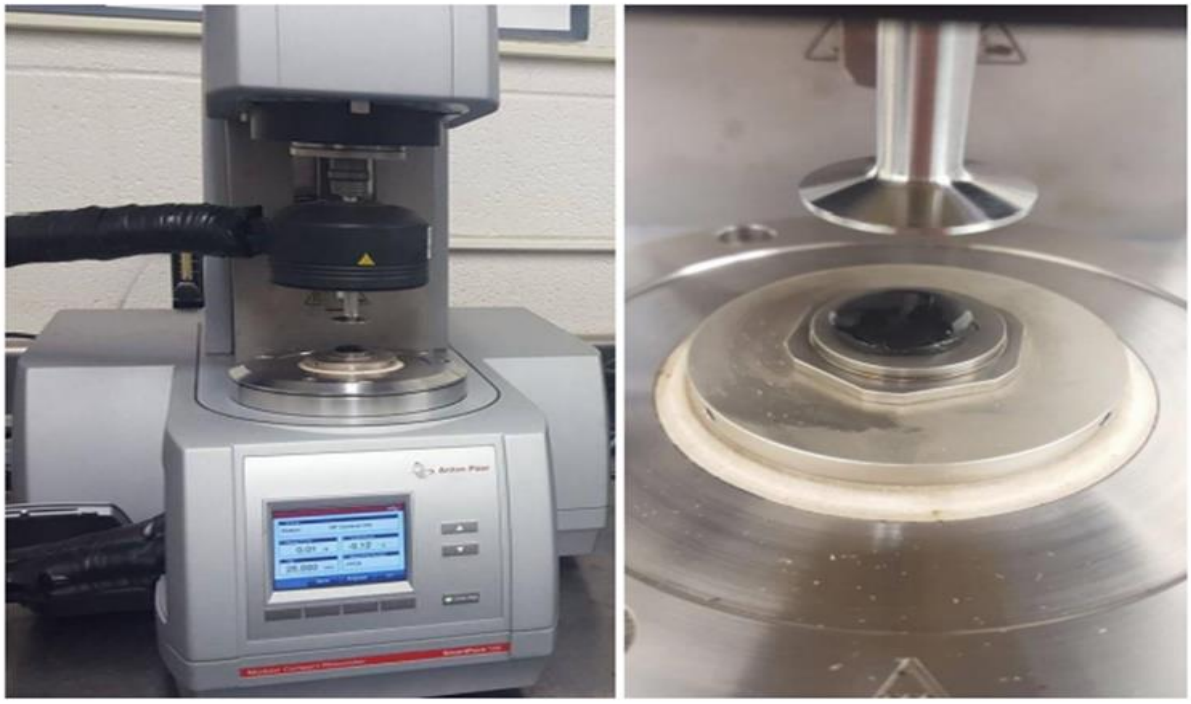

Figure 3.6 Dynamic Shear Rheometer (DSR)

Binders' |G*| and δ values were measured for the original, RTFO-aged, and PAV-aged conditions according to AASHTO 315. The rutting parameter |G*|/sin δ was obtained for the original and RTFO-aged binders, while the fatigue resistance parameter |G*|.sin δ was obtained for the PAV-aged binder.

3.8 Multiple Stress Creep Recovery (MSCR)Test

The MSCR test was conducted on RTFO-aged binders at a specified temperature to characterize the rutting response in asphalt binders. Using a DSR, a 25-mm parallel plate was used with a 1-mm gap. The test was conducted at 58 ºC for the seven binders. The asphalt binder was tested in creep at a percent of the recovery, followed by nonrecoverable creep compliance. The two-stress level used were 0.1 KPa and 3.2 KPa; 20 cycles run at the 0.1 KPa stress level, followed by 10 cycles at the 3.2 KPa stress level for a total of 30 cycles. The creep portion of this test lasts for 1s,

followed by 9s of the recovery period as per AASHTO TP 70 (AASHTO, 2014a). The nonrecoverable creep compliance ($J_{nr)}$ was subsequently obtained.

3.9 Linear Amplitude Sweep (LAS) Test

LAS test was conducted according to AASHTO TP 101 (AASHTO, 2014b), which is based on the simplified viscoelastic continuum damage (S-VECD) analysis method and performed using the DSR. This test was performed on PAV-aged asphalt binder residue. A DSR 8mm parallel plate geometry was used with a 2 mm gap at a temperature of 19 ^{o}C.

LAS test consists of a frequency sweep for estimating undamaged asphalt binder properties and an amplitude sweep. The first test consisted of applying oscillatory shear loadings at twelve various frequencies to measure |G*| and δ. The second test determined the asphalt binder's damage characteristics.

3.10 Predicting Binder |G*| and δ

The procedure for predicting the |G*| and δ is outlaid in the steps below:

1) A and VTS values were obtained according to the binder's performance grade from Table 2.1,
2) For a range of temperatures, the modified ASTM Ai-VTSi model was used to calculate viscosity using Equation 2-4,
3) The |G*| and δ were predicted using Equations 2-5 and 2-6,
4) The predicted |G*| and δ were compared to measured RTFO-aged |G*| and δ,
5) The coefficient of determination (R^2) was used to determine the goodness of fit.

CHAPTER IV

RESULTS AND DISCUSSIONS

4.1 Binder Viscosity

Binder viscosity plays a fundamental role in all three levels of the MEPDG. In addition, the evaluation of a binder's viscosity as it ages indicates a pavement's performance throughout its design life. Table 4.1 illustrates that the viscosity of the eight binders increases with aging. Figure 4.1 presents the same data, which displays a similar trend. The viscosity of the binders was between the ranges of 0.170 ± 0.02 and 0.280 ± 0.03 Pa·s in all projects indicating that the sampled binders will maintain their viscoelasticity even after undergoing long-term aging (ASTM, 2015). However, it was observed that binders with performance grade 58H-34 had higher viscosity values, especially after aging. The binders with PG grade 58H-34 are best suited to resist rutting because of their higher stiffness throughout the aging process.

Table 4.1 Viscosity of Binder for the Eight Projects

			Viscosity at 135^{o}c (mPa.s)		
Project Name	**Location**	**Grading**	**Unaged**	**Short-term aged**	**Long-term aged**
HWY 32	Finley	PG 58S-28	454	841.27	868.80
HWY 32	Finley	PG 58H-34	840	1601.33	2193.00
HWY 83	Minot	PG 58H-34	1602	2215.33	2378.67
HWY 6	Bismarck	PG 58S-34	785	1660.67	2216.67
HWY 28	Minot	PG 58S-28	464	836.63	1080.33
HWY 94	-	PG 58H-34	1507	1801.00	2976.00
HWY 52	Devils Lake	PG 58H-34	1864.33	2305.33	3177
HWY 1	Grand Forks	PG 58H-34	623.77	891.63	1279.67

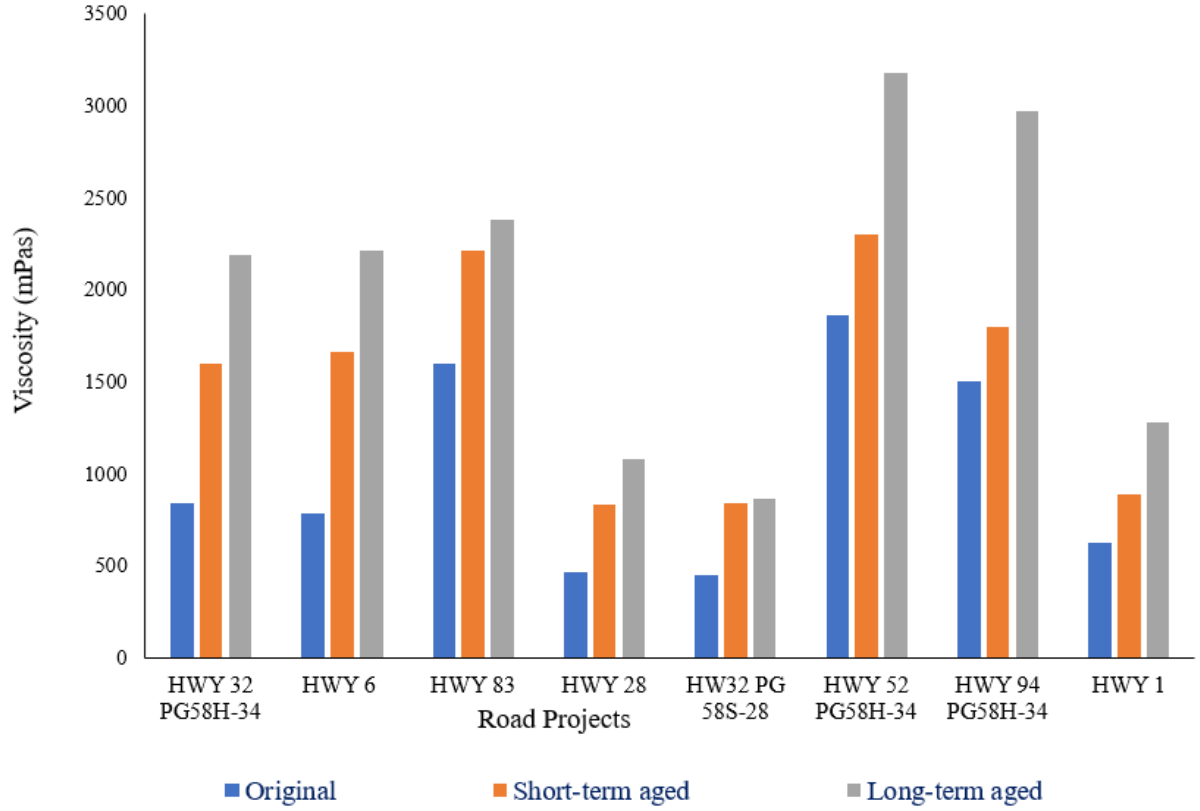

Figure 4.1 Viscosity of Binder for the Eight Projects

4.2 Complex Shear Modulus |G*| and Phase Angle (δ)

The |G*| and associated δ of the eight binders in their original or unaged conditions were measured. Using DSR at a frequency of 10 rad/sec according to AASHTO T315 specifications. Figure 4.2 illustrates that generally, |G*| decreases with an increase in temperature, which means that binders are stiffer at lower temperatures and begin to soften once the temperature increases. An asphalt binder should be stiff and elastic to resist rutting; the parameter G*/sinδ is used to indicate the rutting susceptibility of binders. Fatigue resistance of binder is illustrated using the G*.sinδ parameter from DSR.

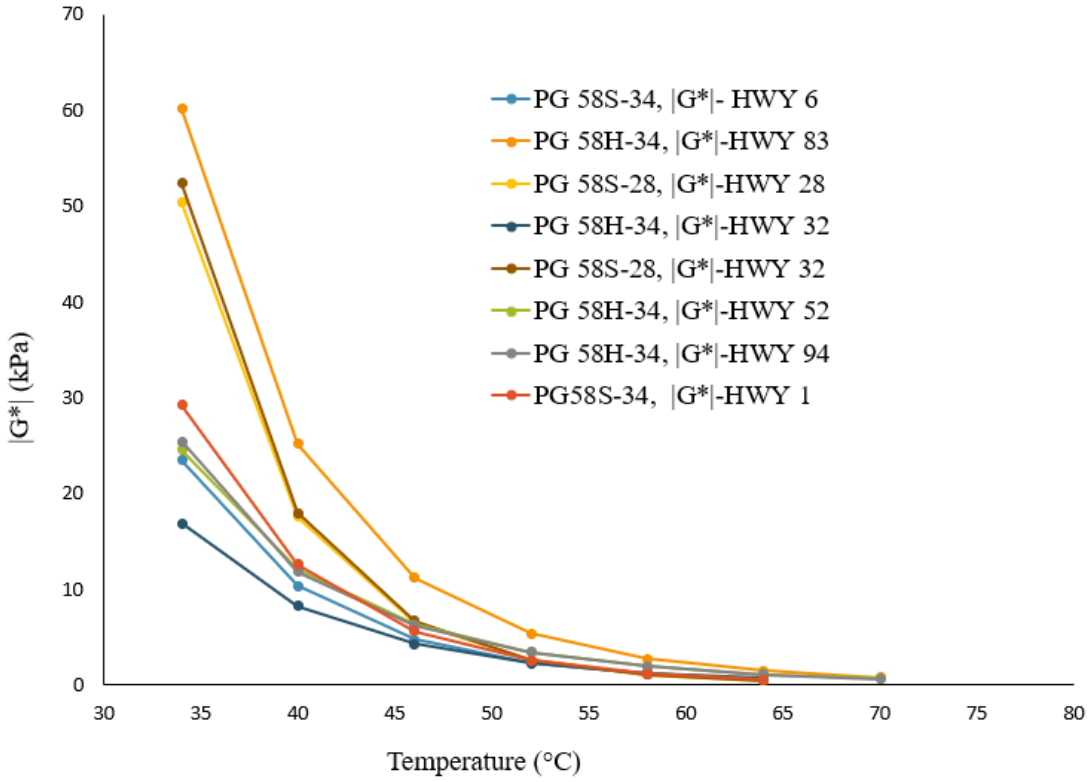

Figure 4.2 Complex Shear Modulus (|G*|) of the Unaged Binder

4.2.1 Original Binder

Tables 4.2 to 4.9 and Figures 4.2 and 4.3 present the original binder DSR test results. For unaged binders, the |G*|/sin(δ) value should be higher than or equal to 1.0 kPa; otherwise, the binder is deemed to have failed at that temperature. The number highlighted red in Tables 4.2 to 4.9 shows the temperature at which the binder failed. The asphalt binder used in HWY 83 PG58H-34 had the highest |G*| values indicating that it could resist rutting up to a temperature of 64ºC. A significant difference was observed with the other binder with the same performance grade of PG58H-34 from HWY 32; it had the lowest |G*| values out of all the binders. The results indicated that the PG58H-34-HWY 32 binder could resist rutting up to 58ºC. This discrepancy illustrates the importance of undertaking local binder characterization to ascertain their performance. It is important to note that all the binders performed satisfactorily at high temperatures according to their performance grade.

Table 4.2 Temperature Sweep Results for Original Binder PG 58S-34 - HWY 6

Temperature (°C)	|G*| (kPa)	Phase Angle (δ)	|G*|/sin(δ) (kPa)
16.00	273.63	64.31	303.69
22.00	142.48	70.36	151.29
28.00	56.39	70.62	59.78
34.00	23.51	70.89	24.88
40.00	10.32	71.43	10.88
46.00	4.80	72.34	5.04
52.00	2.35	73.63	2.45
58.00	1.20	75.23	1.24
64.00	0.64	77.03	0.65

Table 4.3 Temperature Sweep Results for Original Binder PG 58H-34 - HWY 83

Temperature (°C)	|G*| (kPa)	Phase Angle (δ)	|G*|/sin(δ) (kPa)
22.00	381.39	69.71	406.66
28.00	149.89	70.63	158.89
34.00	60.17	70.91	63.67
40.00	25.22	70.86	26.70
46.00	11.24	70.85	11.90
52.00	5.40	71.11	5.71
58.00	2.77	71.59	2.92
64.00	1.48	71.86	1.56
70.00	0.82	71.67	0.86

Table 4.4 Temperature Sweep Results for Original Binder PG 58S-28 - HWY 28

Temperature (°C)	|G*| (kPa)	Phase Angle (δ)	|G*|/sin(δ) (kPa)
16.00	1590.27	68.48	1709.45
22.00	430.39	74.60	446.43
28.00	142.33	77.83	145.60
34.00	50.31	80.71	50.98
40.00	17.61	83.26	17.74
46.00	6.58	85.32	6.60
52.00	2.63	86.87	2.63
58.00	1.12	88.03	1.12
64.00	0.52	88.75	0.52

Table 4.5 Temperature Sweep Results for Original Binder PG 58H-34 - HWY 32

Temperature (°C)	|G*| (kPa)	Phase Angle (δ)	|G*|/sin(δ) (kPa)
22.00	88.73	68.65	95.27
28.00	37.20	67.83	40.17
34.00	16.91	66.98	18.37
40.00	8.28	66.65	9.02
46.00	4.27	67.16	4.63
52.00	2.28	68.56	2.45
58.00	1.24	70.65	1.32
64.00	0.69	73.30	0.73

Table 4.6 Temperature Sweep Results for Original Binder PG 58S-28 - HWY 32

Temperature (°C)	|G*| (kPa)	Phase Angle (δ)	|G*|/sin(δ) (kPa)
16.00	1411.89	66.61	1535.55
22.00	507.93	74.41	527.33
28.00	159.21	78.00	162.77
34.00	52.33	80.93	52.99
40.00	18.00	83.48	18.12
46.00	6.70	85.51	6.72
52.00	2.60	87.04	2.60
58.00	1.11	88.16	1.11
64.00	0.52	88.85	0.52

Table 4.7 Temperature Sweep Results for Original Binder PG 58H-34 - HWY 52

Temperature (°C)	|G*| (kPa)	Phase Angle (δ)	|G*|/sin(δ) (kPa)
34.00	24.57	64.81	27.15
40.00	12.17	64.75	13.46
46.00	6.34	65.22	6.98
52.00	3.45	66.14	3.77
58.00	1.95	67.29	2.11
64.00	1.14	68.43	1.23
70.00	0.69	69.26	0.74

Table 4.8 Temperature Sweep Results for Original Binder PG 58H-34 - HWY 94

Temperature (°C)	|G*| (kPa)	Phase Angle (δ)	|G*|/sin(δ) (kPa)
34.00	24.57	64.81	27.15
40.00	12.17	64.75	13.46
46.00	6.34	65.22	6.98
52.00	3.45	66.14	3.77
58.00	1.95	67.29	2.11
64.00	1.14	68.43	1.23
70.00	0.69	69.26	0.74

Table 4.9 Temperature Sweep Results for Original Binder PG 58S-34 - HWY 1

Temperature (°C)	|G*| (KPa)	Phase Angle (δ)	|G*|/sin(δ) (KPa)
34.00	29.22	74.53	30.31
40.00	12.60	77.09	12.92
46.00	5.61	79.67	5.70
52.00	2.57	82.02	2.60
58.00	1.23	84.00	1.23
64.00	0.61	85.54	0.61

The phase angle (δ) is a parameter that measures the elasticity of a binder. Figure 4.3 illustrates that binders designated as PG 58S-28 had higher δ values and therefore, were less elastic than those designated as PG 58H-34.

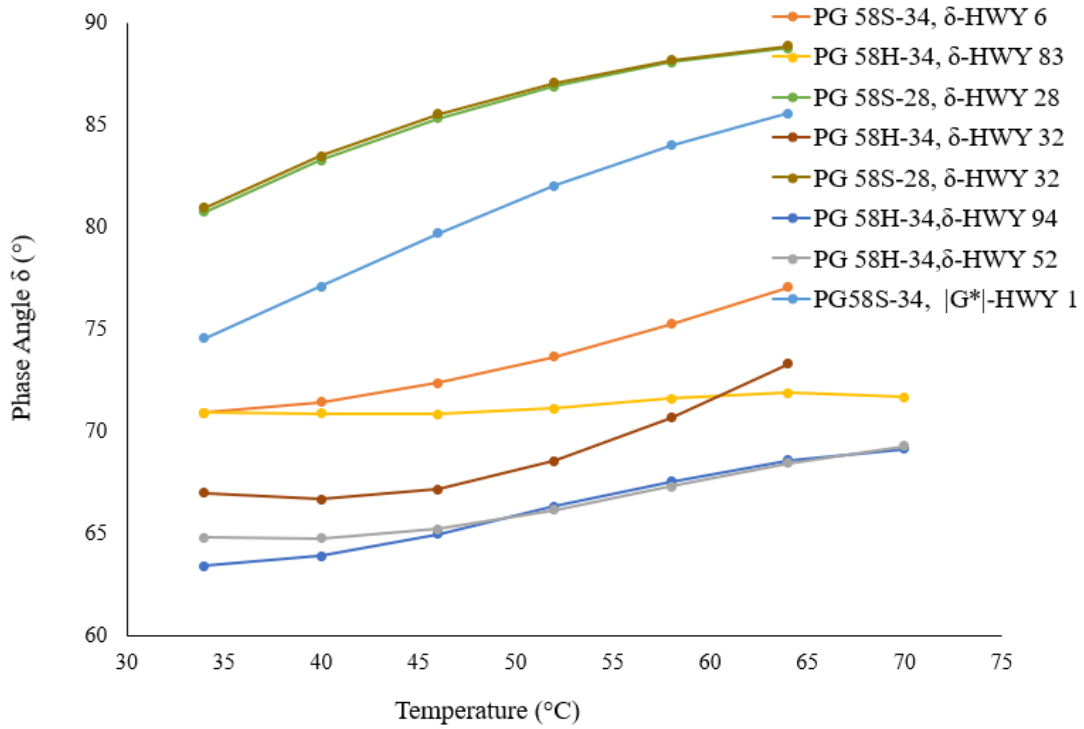

Figure 4.3 Phase Angle (δ) of the Unaged Binder

4.2.2 RTFO-Aged Binder

Short-term aging of the binder was simulated in the laboratory using the RTFO according to AASHTO T240. The RTFO simulates the aging that occurs on the binder during batching, mixing, transportation, and construction of the flexible pavement. The |G*| and δ of the RTFO-aged binders were determined as these are required design inputs in the MEPDG. Figure 4.4 presents the |G*| values of the RTFO-aged binder.

Tables 4.10 to 4.17, and Figures 4.4 and 4.5 present the RTFO aged binder test results. The |G*|/sin(δ) value should be higher than or equal to 2.20 kPa for RTFO-aged binders; otherwise, the binder is deemed to have failed at that temperature. The number highlighted in red in Tables 4.10 to 4.17 shows the temperature at which the binder failed. The results displayed a similar trend to those of the unaged binder. PG 58S-28-HWY 32, PG 58S-28-HWY 28, and PG 58H-34-HWY 83 displayed the highest |G*| values. PG58H-34-HWY 52 had the lowest |G*|. All the binders

failed at the same temperatures as the unaged binder |G*| testing, indicating that although short-term aging has a stiffening effect, the binders' rutting resistance properties remained consistent.

Figure 4.5 illustrates the δ of the RTFO-aged binders. The binders with higher δ values are generally less elastic and it is apparent that these binders are the ones that displayed higher stiffness in Figure 4.5. For binders to resist rutting, they must have higher |G*| to indicate high stiffness and correspondingly lower δ as an indication of the ability to recover after deformation. These characteristics are especially important during an asphalt pavement's early life. PG 58H-34-HWY 83 displayed these characteristics and should be recommended for use in highways anticipating high traffic loads.

Table 4.10 Temperature Sweep Results for RTFO-Aged PG 58S-34 - HWY 6

Temperature (°C)	|G*| (kPa)	Phase Angle (δ)	|G*|/sin(δ) (kPa)
28.00	110.79	65.48	121.77
34.00	48.90	65.29	53.83
40.00	22.55	65.10	24.86
46.00	11.01	65.20	12.13
52.00	5.67	65.80	6.22
58.00	3.03	67.01	3.29
64.00	1.66	68.77	1.78

Table 4.11 Temperature Sweep Results for RTFO-Aged PG 58H-34 - HWY 83

Temperature (°C)	|G*| (kPa)	Phase Angle (δ)	|G*|/sin(δ) (kPa)
34.00	124.42	66.76	135.40
40.00	53.03	67.32	57.47
46.00	23.51	67.84	25.39
52.00	11.04	68.51	11.86
58.00	5.48	69.41	5.86
64.00	2.85	70.60	3.02
70.00	1.52	72.13	1.60

Table 4.12 Temperature Sweep Results for RTFO-Aged PG 58S-28 - HWY 28

Temperature (°C)	|G*| (kPa)	Phase Angle (δ)	|G*|/sin(δ) (kPa)
28.00	289.56	67.20	314.12
34.00	132.69	73.60	138.32
40.00	48.23	76.81	49.54
46.00	18.24	79.92	18.52
52.00	7.25	82.63	7.31
58.00	3.03	84.79	3.05
64.00	1.34	86.47	1.34

Table 4.13 Temperature Sweep Results for RTFO-Aged PG 58H-34 - HWY 32

Temperature (°C)	|G*| (kPa)	Phase Angle (δ)	|G*|/sin(δ) (kPa)
34.00	41.64	63.74	46.43
40.00	20.20	63.07	22.66
46.00	10.37	62.80	11.67
52.00	5.60	63.22	6.27
58.00	3.11	64.47	3.45
64.00	1.75	66.55	1.91

Table 4.14 Temperature Sweep Results for RTFO-Aged PG 58S-28 - HWY 32

Temperature (°C)	|G*| (kPa)	Phase Angle (δ)	|G*|/sin(δ) (kPa)
28.00	320.42	70.22	340.35
34.00	133.02	74.42	138.10
40.00	47.93	77.57	49.08
46.00	17.84	80.60	18.08
52.00	7.04	83.20	7.09
58.00	2.93	85.24	2.94
64.00	1.29	86.85	1.29

Table 4.15 Temperature Sweep Results for RTFO-Aged PG 58H- HWY 52

Temperature (°C)	|G*| (kPa)	Phase Angle (δ)	|G*|/sin(δ) (kPa)
34.00	24.57	64.81	27.15
40.00	12.17	64.75	13.46
46.00	6.34	65.22	6.98
52.00	3.45	66.14	3.77
58.00	1.95	67.29	2.11
64.00	1.14	68.43	1.23
70.00	0.69	69.26	0.74

Table 4.16 Temperature Sweep Results for RTFO-Aged PG 58H- HWY 94

Temperature (°C)	|G*| (kPa)	Phase Angle (δ)	|G*|/sin(δ) (kPa)
34.00	48.85	61.28	55.71
40.00	24.29	61.51	27.64
46.00	12.49	62.01	14.14
52.00	6.66	62.80	7.49
58.00	3.68	63.86	4.10
64.00	2.09	65.15	2.30
70.00	1.21	66.66	1.32

Table 4.17 Temperature Sweep Results for RTFO-Aged PG 58S-34 HWY 1

Temperature (°C)	|G*| (kPa)	Phase Angle (δ)	|G*|/sin(δ) (kPa)
34.00	74.65	68.96	79.98
40.00	32.25	71.44	34.02
46.00	14.20	74.20	14.75
52.00	6.43	76.97	6.60
58.00	2.97	79.59	3.02
64.00	1.42	81.90	1.44

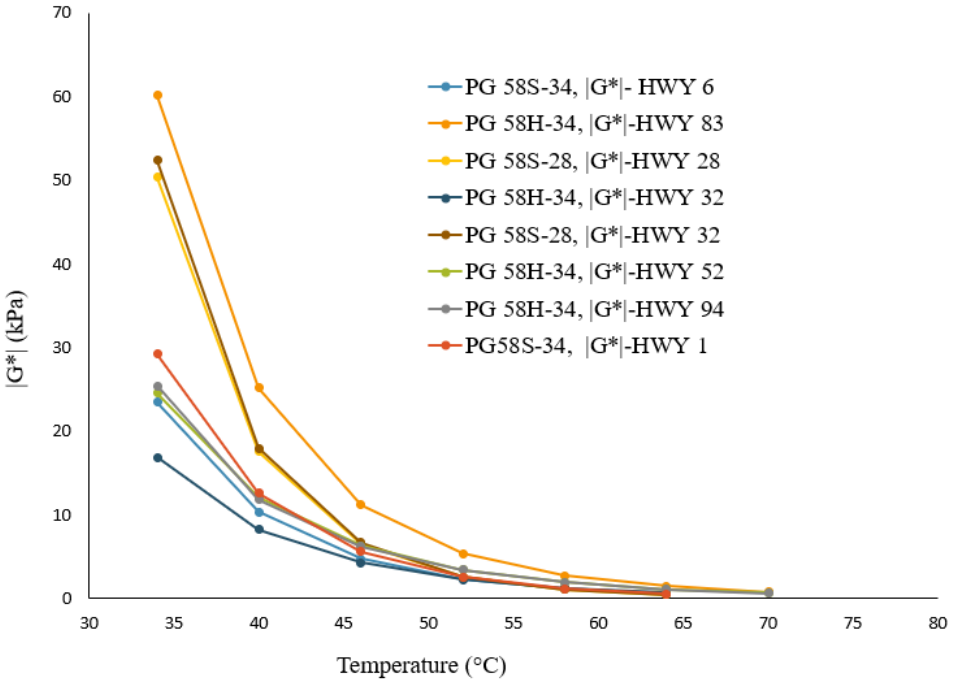

Figure 4.4 Complex Shear Modulus (|G*|) of the RTFO-Aged Binder

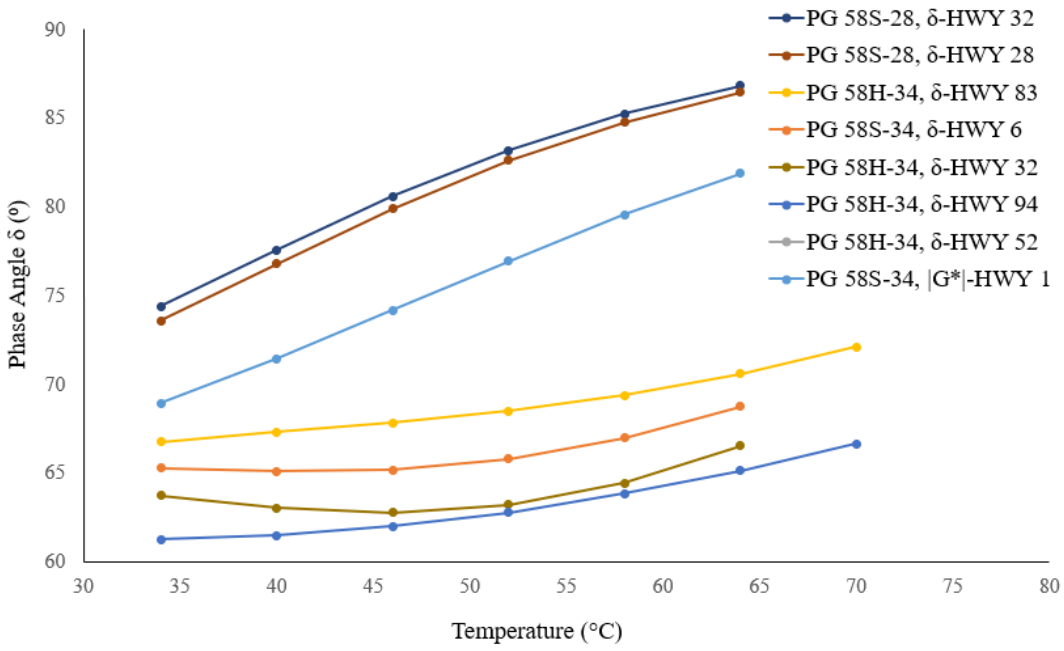

Figure 4.5 Phase Angle (δ) of the RTFO-Aged Binder

4.2.3 PAV-Aged Binder

Asphalt pavements begin to experience fatigue cracking at the later stages of their design life; therefore, it is important to determine and evaluate binder properties after undergoing long-term aging. The PAV is intended to simulate the long-term aging of the binder by exposing the binder to an elevated temperature in a pressurized chamber. The eight asphalt binders were first conditioned in the RTFO before the residues were conditioned further in the PAV. This long-term oxidative aging occurs in asphalt binders during pavement service. The PAV simulates 5 to 10 years of in-service aging of the asphalt binder (AASHTO, 2021a). The |G*| and δ of the PAV-aged binders are illustrated in Figures 4.6 to 4.7. For PAV-aged binders, the binder should be elastic and less stiff to avoid cracking.

Tables 4.18 to 4.25 and Figures 4.6 to 4.7 present the PAV-aged binder test results. The parameter used as a threshold value is the |G*|. sin(δ), which should be less than 5000 kPa; otherwise, the binder is deemed to have failed at that temperature. The number highlighted in red in Tables 4.18 to 4.25 shows the temperature at which the binder failed.

Table 4.18 Temperature Sweep Results for PAV-Aged PG 58S-28 - HWY 32

Temperature (°C)	|G*| (kPa)	Phase angle δ (°)	|G*|·sin(δ) (kPa)
22.00	1243.39	63.49	1112.57
19.00	2229.77	60.21	1934.93
16.00	3849.25	56.83	3221.66
13.00	6500.04	53.26	5208.68

Table 4.19 Temperature Sweep Results for PAV-Aged PG 58S-34 - HWY 6

Temperature (°C)	|G*| (kPa)	Phase angle δ (°)	|G*|·sin(δ) (kPa)
22.00	469.57	61.99	414.28
19.00	789.48	60.82	688.70
16.00	1327.80	59.33	1140.97
13.00	2235.38	57.52	1470.49
10.00	3763.44	55.37	3093.81
7.00	6312.51	52.93	5031.12

Table 4.20 Temperature Sweep Results for PAV-Aged PG 58H-34 - HWY 32

Temperature (°C)	|G*| (kPa)	Phase angle δ (°)	|G*|·sin(δ) (kPa)
22.00	353.23	60.83	309.83
19.00	583.94	59.68	507.43
16.00	960.48	58.17	823.48
13.00	1583.94	56.26	1333.01
10.00	1624.61	54.01	2155.40
7.00	4328.47	51.45	3446.60
4.00	7058.58	25.03	5415.56

Table 4.21 Temperature Sweep Results for PAV-Aged PG 58H-34 - HWY 83

Temperature (°C)	|G*| (kPa)	Phase angle δ (°)	|G*|·sin(δ) (kPa)
22.00	959.68	59.67	827.78
19.00	1656.70	57.17	1391.07
16.00	2782.65	54.60	2266.02
13.00	3983.24	51.87	3598.54
10.00	7461.99	48.90	5616.05

Table 4.22 Temperature Sweep Results for PAV-Aged PG 58H-34 - HWY 28

Temperature (°C)	|G*| (kPa)	Phase angle δ (°)	|G*|·sin(δ) (kPa)
22.00	1211.75	63.83	1142.80
19.00	2152.31	60.60	1997.53
16.00	3666.10	57.27	3338.44
13.00	6128.85	53.70	5453.37

Table 4.23 Temperature Sweep Results for PAV-Aged PG 58H-34 - HWY 52

Temperature (°C)	|G*| (kPa)	Phase angle δ (°)	|G*|·sin(δ) (kPa)
22.00	210.68	58.03	178.86
19.00	332.20	56.91	278.53
16.00	523.41	55.53	431.84
13.00	826.75	53.90	668.56
10.00	1303.56	52.05	1028.88
7.00	2043.08	50.04	1567.71
4.00	3174.51	47.92	2358.87
1.00	4903.69	45.66	3512.46
-2.00	7468.53	43.37	5137.36

Table 4.24 Temperature Sweep Results for PAV-Aged PG 58H-34 - HWY 94

Temperature (°C)	|G*| (kPa)	Phase angle δ (°)	|G*|·sin(δ) (kPa)
19.00	663.43	54.88	595.00
16.00	1143.13	53.25	915.93
13.00	1778.12	51.48	1391.16
10.00	2755.56	49.51	2095.47
7.00	4270.85	47.38	2607.05
4.00	6542.19	45.13	4636.52
1.00	9908.15	42.82	6734.29

Table 4.25 Temperature Sweep Results for PAV-Aged PG 58S-34 - HWY 1

Temperature (°C)	|G*| (kPa)	Phase angle δ (°)	|G*|·sin(δ) (kPa)
22.00	476.07	61.64	324.70
19.00	792.67	60.25	533.13
16.00	1294.99	58.61	861.10
13.00	2104.96	56.68	1385.58
10.00	3424.55	54.46	2212.27
7.00	5497.83	51.97	3491.06
4.00	8767.47	49.27	5436.87

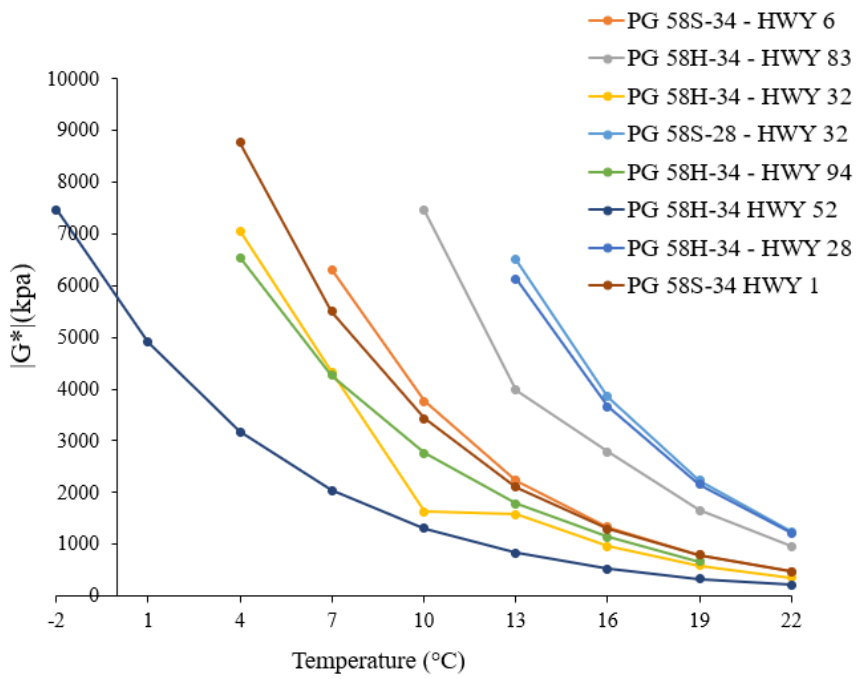

Figure 4.6 Complex Shear Modulus (|G*|) of the PAV-Aged Binder

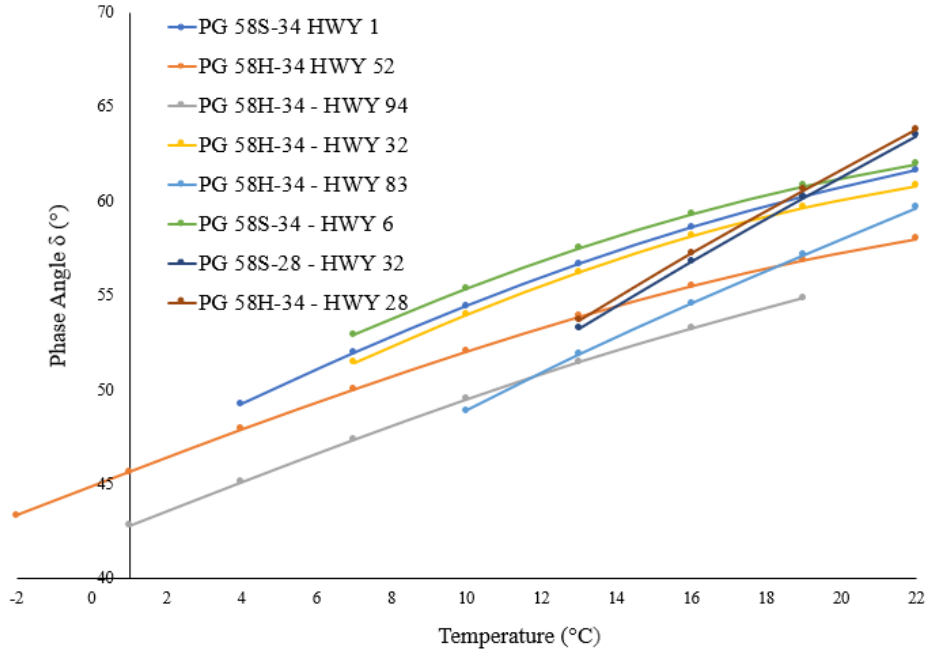

Figure 4.7 Phase Angle (δ) of the PAV-Aged Binder

PG 58H-34-HWY 52 had a |G*|. sin(δ) value that was less than 5000 kPa at -2ºC, PG 58H-34-HWY 94 at 1ºC and PG 58H-34-HWY 32 at 7ºC. The rest of the binders were above the threshold value at this temperature, indicating that PG 58H-34-HWY 52, PG 58H-34-HWY 94, PG 58S-34-HWY 1 and PG 58H-34-HWY 32 binders are the least susceptible to fatigue ranking. PG 58H-34 - HWY 28 and PG 58S-28 - HWY 32 failed to meet the threshold at 16ºC, indicating they are more susceptible to fatigue cracking.

4.3 Binder Ranking

Table 4.26 presents results for five asphalt binders under four testing parameters. The first parameter specifies a maximum value of 5000 kPa for G*.sinδ values measured from DSR tests conducted on PAV-aged asphalt binders and measures fatigue resistance. The second parameter used the RTFO-aged binder test results to get the parameter |G*|/sin(δ) value, which should be higher than or equal to 2.20 kPa, which indicates the rutting resistance of the binder. The third and fourth parameters, MSCR and LAS, were used to evaluate the rutting and fatigue resistance of the asphalt binder, respectively. Table 4.26 shows all test results for five binders. Based on the test results in Table 4.26, the binders were ranked from A to E; the binders' rutting and fatigue resistance were ranked differently under different binder tests.

Table 4.26 Test Results of Five Binders

Tests	Important information	PG58H-34 HWY 32	PG58S-34 HWY 6	PG58H-34 HWY 94	PG58H-34 HWY 52	PG58S-34 HWY 1
LAS	Parameter A	24735970.49	4540515.55	66012308.37	25920029.00	215759.33
	Parameter B	-4.79	-4.70	-5.09	-4.99	-2.93
	Fatigue life at N_f=2.5%	304281.27	61390.50	622600.75	267818.40	14822.03
	Fatigue life at N_f=5%	10927.75	2367.32	18291.38	8426.45	1954.73
	Overall ranking	B	D	A	C	E
MSCR	Test temperature (°C)	58	58	58	58	58
	Percent non-recovery- J nr(0.1kpa)	0.65	1.21	0.31	0.36	2.51
	Percent non-recovery J_nr(3.2kpa)	1.10	2.47	0.63	1.01	3.28
	Percent difference of non-recoverable J_nr_diff	71.14	104.68	100.51	181.36	15.17
	Overall ranking	B	D	C	E	A
|G*|·sin(δ) (KPa)	Test temperature (°C)	4	7	1	-1	4
	|G*|·sin(δ)	5415.56	5031.12	6734.29	5137.37	5436.87
	Overall ranking	D	E	B	A	C
|G*|/sin(δ) (KPa)	Test temperature (°C)	64.00	64.00	64.00	64.00	64.00
	|G*|/sin(δ)	1.91	1.78	1.12	1.23	1.44
	Overall ranking	E	D	A	B	C

Note: Asphalt binders are ranked from A to E, A refers to the best, and E is the last one

4.3.1 Fatigue Resistance of Binder Ranking

For fatigue resistance ranking |G*|. sinδ and LAS test results were used. |G*|. sinδ shows the temperature that corresponds to 5000 kPa. Generally, the lowest temperature indicated the best fatigue resistance. Table 4.26 illustrates that the binder used in PG 58H-34 - HWY 52 has good resistance to fatigue cracks and ranked the best, followed by PG 58H-34 - HWY 94, while PG 58S-34 - HWY 6 performed poorly and was ranked E.

LAS ranking was also used to rank the binder according to their fatigue resistance. Table 4.24 shows that the binder used in PG 58H-34 - HWY 94 has good resistance to fatigue cracks and is ranked the best, followed by PG 58H-34 - HWY 32 and PG 58S-34 - HWY 1 performed poorly and ranked E.

4.3.2 Rutting Resistance of Binder Ranking

Rutting resistance |G*|/sin(δ) and MSCR test results were used for ranking the binders. For |G*|/sin(δ), the correlation was done for 64^{o}C, PG 58H-34 - HWY 94 resisted rutting at 64^{o}C better than the four binders and ranked A. PG 58H-34 HWY 32 performed poor at 64^{o}C; therefore; it ranked E.

MSCR test ranking shows that according to their rutting resistance, the percent difference of nonrecoverable result illustrate that PG 58S-34 HWY 1 has good resistance for rutting and ranked A while PG 58H-34 HWY 52 performed poorly the last and ranked E.

4.4 Comparison of Measured and Predicted Binder Properties

Laboratory-measured |G*| and δ for the RTFO-aged binder are required inputs for levels 1 and 2 of the MEPDG; these values are then converted to viscosity at various temperatures. The MEPDG measurements use default A and VTS parameters to estimate binder viscosity for level 3 (Bari & Witczak, 2007). Pavement projects have varying reliability requirements and measuring the |G*|

and (δ) of asphalt binders is costly and time-consuming. Predicting these parameters using existing models can provide a useful tool for pavement engineers.

|G*| and δ were predicted using predictive models. By inputting the default, A and VTS values shown in Table 2.1 into Equations 2-4, 2-5, and 2-6 to generate viscosity, |G*|, and δ. Then the predicted results were compared with laboratory-measured |G*| and δ for the short-term aged binder.

Figure 4.8 compares the predicted |G*| with the RTFO-aged |G*| for the eight binders under study. A good correlation was observed between the measured and predicted values with an R^2 higher than 0.9 for all binders. However, the model consistently underestimated the |G*| values as indicated by the trendline, especially at higher temperatures.

Figure 4.9 presents a comparison of the predicted and measured δ values. The results were mixed with PG 58S-28-HWY 32, PG 58H-34-HWY 83, PG58S-28-HWY 28, and PG 58S-34-HWY 1, displaying good correlations with R^2 values higher than 0.9 and PG 58H-34-HWY 52 and PG 58H-34-HWY 94 also shows good correlation R^2 values higher than 0.8; however, PG58S-34-HWY 6 and PG58H-34-HWY 32 displayed poor correlation with R^2 values lower than 0.5. The model overpredicted the results.

Default A and VTS parameters were used to compute viscosity values, which were then used to predict |G*| and δ values: therefore, the accuracy of these parameters is a significant determinant of the model's output. In our case, the model underestimated the |G*| values and overestimated the δ values, with some binders displaying poor agreement with measured δ values. This could be attributed to using the default A and VTS parameters as inputs in the prediction equations. The default A and VTS values were generated based on extensive binder testing undertaken under the

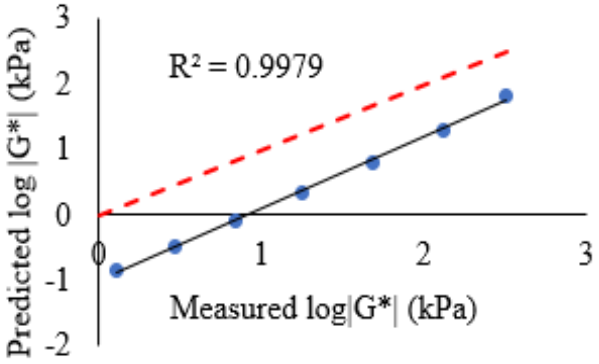
R² = 0.9979
Predicted log |G*| (kPa)
Measured log|G*| (kPa)
3
2
1
0
-1
-2
0
1
2
3

(a)

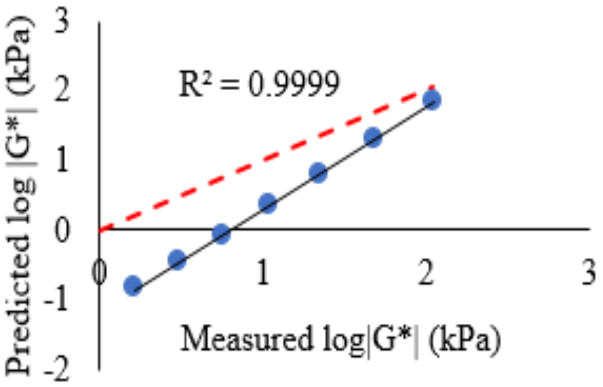
R² = 0.9999
Predicted log |G*| (kPa)
Measured log|G*| (kPa)
3
2
1
0
-1
-2
0
1
2
3

(b)

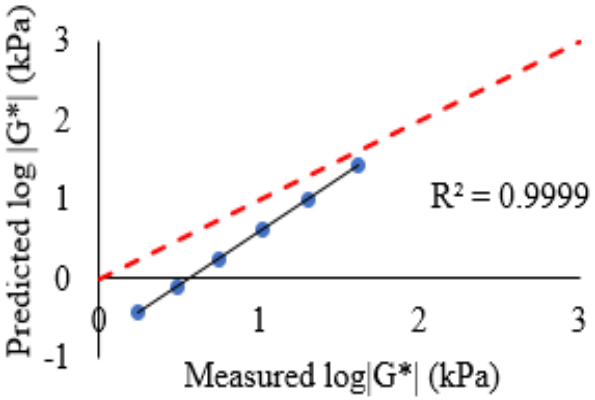
R² = 0.9999
Predicted log |G*| (kPa)
Measured log|G*| (kPa)
3
2
1
0
-1
0
1
2
3

(c)

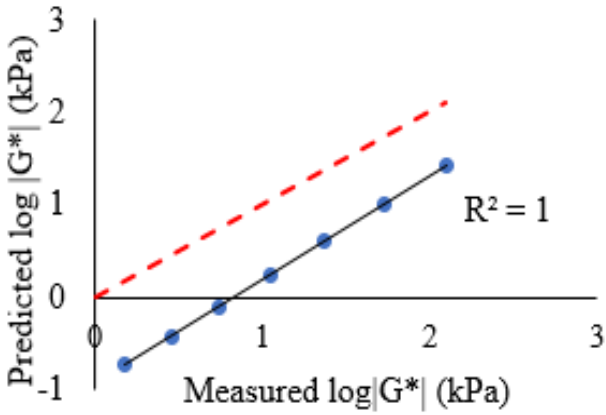
R² = 1
Predicted log |G*| (kPa)
Measured log|G*| (kPa)
3
2
1
0
-1
0
1
2
3

(d)

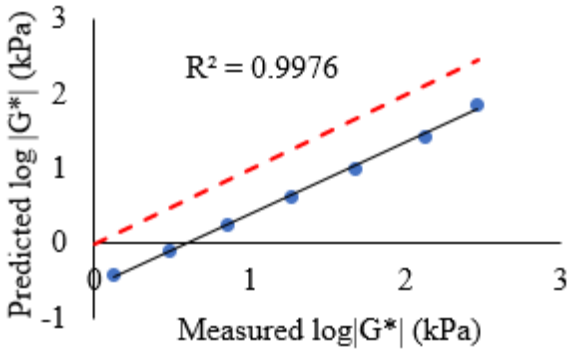

(e)

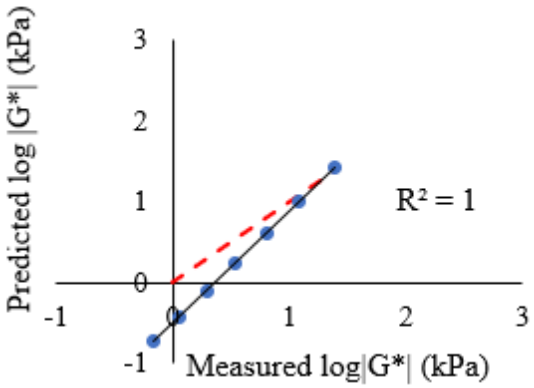

(f)

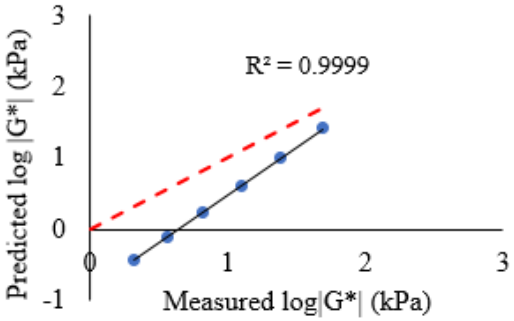

(g)

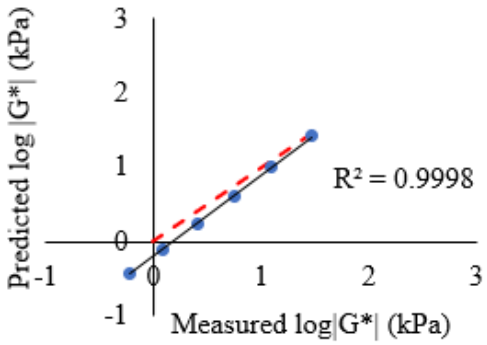

(h)

Figure 4.8 Predicted vs. Measured |G*|:(a) PG 58S-28-HWY 32, (b) PG 58S-34-HWY 6, (c) PG 58H-34-HWY 32, (d) PG 58H-34-HWY 83, (e) PG 58S-28-HWY 28, (f) PG 58H-34-HWY 52 (g) PG 58H-34-HWY 94, (h) PG 58S-34-HWY 1.

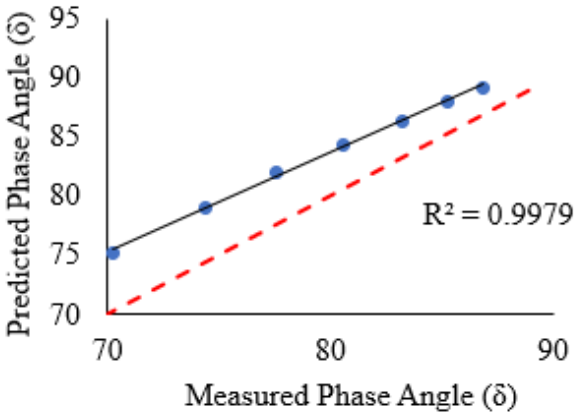
Predicted Phase Angle (δ)
95
90
85
80
75
70
70
80
90
Measured Phase Angle (δ)
R² = 0.9979

(a)

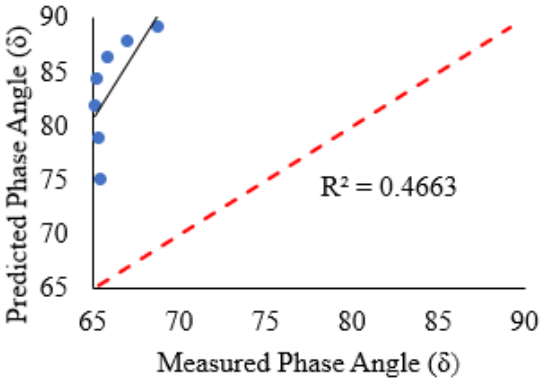
Predicted Phase Angle (δ)
90
85
80
75
70
65
65
70
75
80
85
90
Measured Phase Angle (δ)
R² = 0.4663

(b)

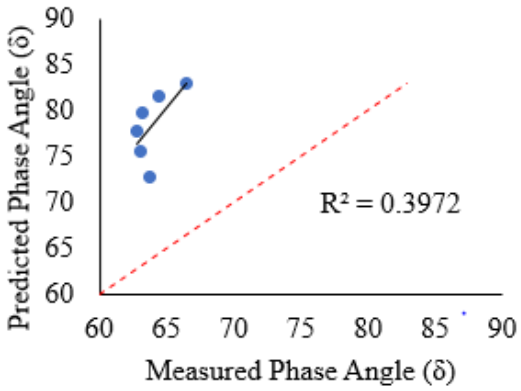
Predicted Phase Angle (δ)
90
85
80
75
70
65
60
60
65
70
75
80
85
90
Measured Phase Angle (δ)
R² = 0.3972

(c)

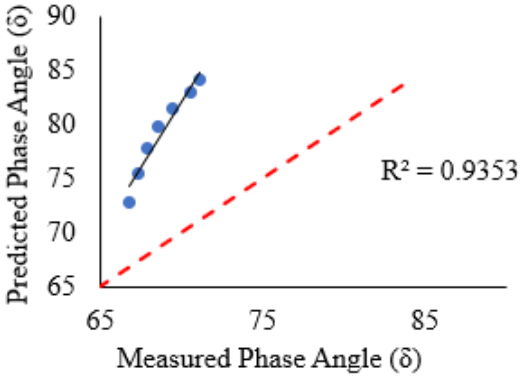
Predicted Phase Angle (δ)
90
85
80
75
70
65
65
75
85
Measured Phase Angle (δ)
R² = 0.9353

(d)

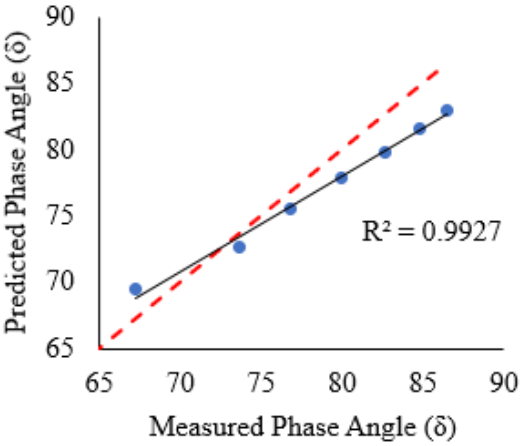
Predicted Phase Angle (δ)
90
85
80
75
70
65
65
70
75
80
85
90
Measured Phase Angle (δ)
R² = 0.9927

(e)

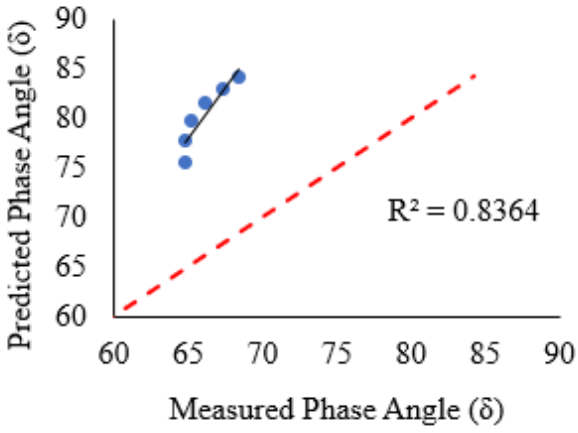
Predicted Phase Angle (δ)
90
85
80
75
70
65
60
60
65
70
75
80
85
90
Measured Phase Angle (δ)
R² = 0.8364

(f)

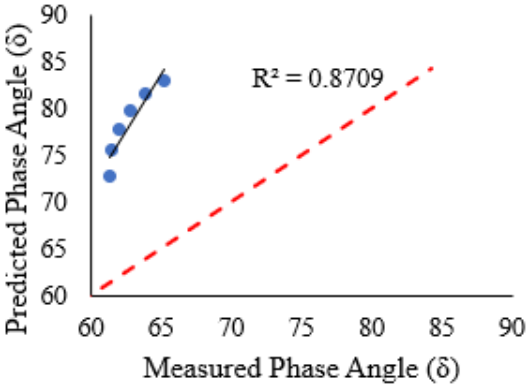

(g)

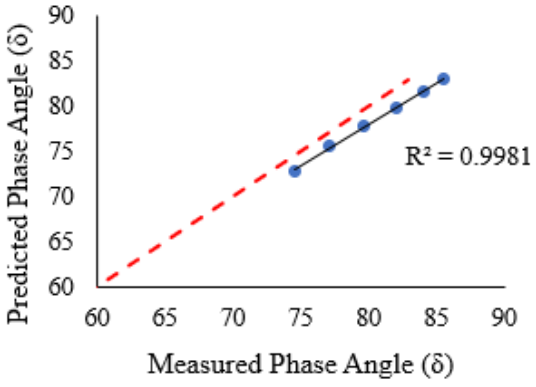

(h)

Figure 4.9 Predicted vs. Measured δ: (a) PG 58S-28-HWY 32, (b) PG 58S-34-HWY 6, (c) PG 58H-34-HWY 32, (d) PG 58H-34-HWY 83, (e) PG 58S-28-HWY 28, (f) PG 58H-34-HWY 52 (g) PG 58H-34-HWY 94, (h) PG 58S-34-HWY 1.

CHAPTER V

CONCLUSIONS, RECOMMENDATIONS, LIMITATIONS, AND FUTURE WORK

5.1 Conclusions

1) The measured viscosity of the binders was between the ranges of 0.170 ± 0.02 and 0.280 ± 0.03 Pa·s in all projects indicating that the sampled binders maintained their viscoelasticity even after undergoing long-term aging. However, binders with performance grade 58H-34 had higher viscosity values, especially after aging. The binders with PG grade 58H-34 are stiffer and are best suited to resist rutting. This explains their higher stiffness through the aging process.
2) The |G*| testing for the unaged binder revealed that the asphalt binder used in HWY 83, PG58H-34, had the highest |G*| values and that it could resist rutting up to a temperature of 64ºC. A significant difference was observed with the other binder with the same performance grade of PG58H-34 from HWY 32; it had the lowest |G*| values out of all the binders. The results demonstrated that the PG58H-34-HWY 32 binder could resist rutting up to 58ºC. This discrepancy illustrates the importance of undertaking local binder characterization to ascertain its performance. It is important to note that all the binders performed satisfactorily at high temperatures according to their performance grade.

   Binders designated as PG 58S-28 had higher δ values and therefore, were less elastic than those designated as PG 58H-34.
3) The |G*| results for the RTFO-aged binders displayed a similar trend to those of the unaged binder. PG 58S-28-HWY 32, PG 58S-28-HWY 28, and PG 58H-34-HWY 83 displayed the highest |G*| values. PG 58H-34-HWY 52 had the lowest |G*|. All the binders failed at the same temperatures as the unaged binder, indicating that although short-term aging has

a stiffening effect, the binders' viscoelastic properties remained consistent. PG 58H-34-HWY 83 displayed should be recommended for use in highways anticipating high traffic loads because of its high |G*| and low δ.

4) PAV-aged binder testing revealed that PG 58H-34-HWY 32 and PG 58H-34-HWY 83 had the highest |G*| values indicating that these binders underwent significant stiffening after long-term aging. PG 58H-34-HWY 52 displayed the lowest |G*|, indicating less sensitivity to aging.
5) Comparing the predicted |G*| with the RTFO-aged |G*| for the eight binders revealed a good correlation between the measured and predicted values with an R^2 higher than 0.9 for all binders. However, the model consistently underestimated the |G*| values, especially at higher temperatures.

   A comparison between the predicted and measured δ values revealed that PG 58S-28-HWY 32, PG 58H-34-HWY 83, PG58S-28-HWY 28 and PG 58S-34-HWY 1 had good agreement with measured values with R^2 higher than 0.9 and PG 58H-34-HWY 52 and PG 58H-34-HWY 94 also shows good correlation R^2 values higher than 0.8; however, PG 58S-34-HWY 6 and PG 58H-34-HWY 32 displayed poor correlation with R^2 values lower than 0.5. The model overpredicted the δ results.
6) Using the |G*|/sinδ parameter showed that PG 58H-34-HWY 94 had the highest rutting resistance, while the MSCR test showed that PG 58S-34-HWY 1 was the most rutting-resistant binder. |G*|. sin(δ) parameter indicated that PG58H-34-HWY 52 had the highest fatigue resistance, while the LAS indicated that PG 58H-34-HWY 94 had the highest fatigue resistance. There was poor agreement between the binder grading results and the MSCR and LAS results.

5.2 Recommendations

Based on this study, the following recommendations can be made:

- Recommend generating A and VTS values for local binders to improve the predictions of the |G*| and δ and provide a substitute for laboratory measurements.
- Asphalt binders were ranked under different binder tests. Studies have shown that the LAS and MSCR tests are superior to the Superpave parameters |G*|. sin(δ) and |G*|/sin(δ). Therefore, further investigation is needed to evaluate the discrepancy obtained in these tests.

5.3 Limitations

Default A and VTS parameters were used to compute viscosity values, which were then used to predict |G*| and δ values: therefore, the accuracy of these parameters is a significant determinant of the model's output. The model underestimated the |G*| values and overestimated the δ values, with some binders displaying poor agreement with measured δ values. This could be attributed to using the default A and VTS parameters as inputs in the prediction equations.

MSCR and LAS tests were conducted for five binders to preliminarily compare their results to binder grading results.

5.4 Future Work

The experiments were conducted on seven binders. By the end of the study, three more binders will be evaluated, which will be more representative of binder properties in North Dakota. MSCR and LAS tests will be conducted to rank the binders according to rutting and fatigue cracking (Johnson & Bahia, 2010).

Reference

AASHTO. (2014a). AASHTO TP 70-14: Standard Method of Test for Multiple Stress Creep Recovery (MSCR) Test of Asphalt Binder Using a Dynamic Shear Rheometer (DSR). American Association of State Highway and Transportation Officials.

AASHTO. (2014b). AASHTO TP 101-14: Estimating Damage Tolerance of Asphalt Binders Using the Linear Amplitude Sweep. American Association of State Highway and Transportation Officials.

AASHTO. (2020). AASHTO T 315-20 Standard Method of Test for Determining the Rheological Properties of Asphalt Binder Using a Dynamic Shear Rheometer (DSR). American Association of State Highway and Transportation Officials.

AASHTO. (2021a). AASHTO R 28-21:Standard Practice for Accelerated Aging of Asphalt Binder Using a Pressurized Aging Vessel (PAV). American Association of State Highway and Transportation Officials.

AASHTO. (2021b). AASHTO T 240-21: Standard Method of Test for Effect of Heat and Air on a Moving Film of Asphalt (Rolling Thin-Film Oven Test). American Association of State Highway and Transportation Officials.

Apeagyei, A. K., & Diefenderfer, S. D. (2011). Asphalt material design inputs for use with the mechanistic-empirical pavement design guide in Virginia. Virginia Center for Transportation Innovation and Research.

ARA, INC. (2004). Guide for Mechanistic–Empirical Design of New and Rehabilitated Pavement Structures. Final Rep., NCHRP Project 1-37A.

ASTM. (2015). ASTM D4402-06: Standard Test Method for Viscosity Determination of Asphalt at Elevated Temperatures Using a Rotational Viscometer. ASTM International.

Awed, A., El-Badawy, S., Bayomy, F., & Santi, M. (2011). Influence of the MEPDG binder characterization input level on the predicted dynamic modulus for Idaho asphalt concrete mixtures. In Proceedings of the Transportation Research Board 90th Annual Meeting, 23–27.

Bari, J., & Witczak, M. W. (2007). New predictive models for viscosity and complex shear modulus of asphalt binders: For use with mechanistic-empirical pavement design guide. Transportation Research Record, 2001(1), 9–19.

Birgisson, B., Roque, R., Kim, J., & Pham, L. V. (2004). The use of complex modulus to characterize the performance of asphalt mixtures and pavements in Florida.

Colbert, B., & You, Z. (2012). The properties of asphalt binder blended with variable quantities of recycled asphalt using short term and long-term aging simulations. Construction and Building Materials, 26(1), 552–557. https://doi.org/10.1016/j.conbuildmat.2011.06.057

D'Angelo, J., Kluttz, R., Dongre, R. N., Stephens, K., & Zanzotto, L. (2007). Revision of the superpave high temperature binder specification: The multiple stress creep recovery test (with discussion). Journal of the Association of Asphalt Paving Technologists, 76.

Dondi, G., Vignali, V., Pettinari, M., Mazzotta, F., Simone, A., & Sangiorgi, C. (2014). Modeling the DSR complex shear modulus of asphalt binder using 3D discrete element approach. Construction and Building Materials, 54, 236–246. https://doi.org/10.1016/j.conbuildmat.2013.12.005

FHWA. (2011). In Multiple Stress Creep Recovery (MSCR) Procedure.

Gedafa, D. S., Hossain, M., Romanoschi, S., & Gisi, A. J. (2010). Field Verification of Superpave Dynamic Modulus. Journal of Materials in Civil Engineering, 22(5), 485–494. https://doi.org/10.1061/(ASCE)MT.1943-5533.0000048

Ghuzlan, K. A., & Al-Khateeb, G. G. (2013). Selection and verification of performance grading for asphalt binders produced in Jordan. International Journal of Pavement Engineering, 14(2), 116–124. https://doi.org/10.1080/10298436.2011.650697

Hintz, C., & Bahia, H. (2013). Simplification of Linear Amplitude Sweep Test and Specification Parameter. Transportation Research Record: Journal of the Transportation Research Board, 2370(1), 10–16. https://doi.org/10.3141/2370-02

Hossain, E. I., Singh, D., & Zaman, P. E. (2013). Dynamic Modulus-based Field Rut Prediction Model from an Instrumented Pavement Section. Procedia - Social and Behavioral Sciences, 104, 129–138. https://doi.org/10.1016/j.sbspro.2013.11.105

Hossain E.I., N., Singh, D., & Zaman P.E., M. (2013). Dynamic Modulus-based Field Rut Prediction Model from an Instrumented Pavement Section. Procedia - Social and Behavioral Sciences, 104, 129–138. https://doi.org/10.1016/j.sbspro.2013.11.105

Johnson, C., & Bahia, H. U. (2010). Evaluation of an accelerated procedure for fatigue characterization of asphalt binders. Submitted for Publication in Road Materials and Pavement Design.

Li, Q. J., Wang, K. C. P., Yang, G., Zhan, J. Y., & Qiu, Y. (2019). Data needs and implementation of the Pavement ME Design. Transportmetrica A: Transport Science, 15(1), 135–164. https://doi.org/10.1080/23249935.2018.1504254

Li, Q., Xiao, D. X., Wang, K. C. P., Hall, K. D., & Qiu, Y. (2011). Mechanistic-empirical pavement design guide (MEPDG): A bird's-eye view. Journal of Modern Transportation, 19(2), 114–133. https://doi.org/10.1007/BF03325749

Mohammad, L. N., Kim, M., Raghavendra, A., & Obulareddy, S. (2014). Characterization of Louisiana asphalt mixtures using simple performance tests and MEPDG. Louisiana. Dept. of Transportation and Development.

Wang, H.-P., Guo, Y.-X., Wu, M.-Y., Xiang, K., & Sun, S.-R. (2021). Review on structural damage rehabilitation and performance assessment of asphalt pavements. REVIEWS ON ADVANCED MATERIALS SCIENCE, 60(1), 438–449. https://doi.org/10.1515/rams-2021-0030

Yao, H., You, Z., Li, L., Shi, X., Goh, S. W., Mills-Beale, J., & Wingard, D. (2012). Performance of asphalt binder blended with non-modified and polymer-modified nanoclay. Construction and Building Materials, 35, 159–170. https://doi.org/10.1016/j.conbuildmat.2012.02.056

Yu, H., & Shen, S. (2013). A micromechanical based three-dimensional DEM approach to characterize the complex modulus of asphalt mixtures. Construction and Building Materials, 38, 1089–1096. https://doi.org/10.1016/j.conbuildmat.2012.09.036

Yusoff, N. I. Md., Shaw, M. T., & Airey, G. D. (2011). Modelling the linear viscoelastic rheological properties of bituminous binders. Construction and Building Materials, 25(5), 2171–2189. https://doi.org/10.1016/j.conbuildmat.2010.11.086

Zeiada, W., Liu, H., Ezzat, H., Al-Khateeb, G. G., Shane Underwood, B., Shanableh, A., & Samarai, M. (2022). Review of the Superpave performance grading system and recent developments in the performance-based test methods for asphalt binder characterization. Construction and Building Materials, 319, 126063. https://doi.org/10.1016/j.conbuildmat.2021.126063

Zhang, Z., Leidy, J. P., Kawa, I., & Ronald Hudson, W. (2000). Impact of Changing Traffic Characteristics and Environmental Conditions on Flexible Pavements. Transportation Research Record: Journal of the Transportation Research Board, 1730(1), Article 1. https://doi.org/10.3141/1730-15